

Electronic Supplementary Information

Time-resolved Control of Nanoparticle Integration in Titanium-Organic Frameworks for Enhanced Catalytic Performance

Carmen Fernández-Conde, Yongkun Zheng, Marta Mon, Antonio Ribera, Antonio Leyva-Pérez and Carlos Martí-Gastaldo

Table of contents

S1. General considerations: starting materials and characterization	S4
Materials and reagents	S4
Structural and chemical characterization	S4
S2. Time-resolved Synthesis of MUV-10 (Ca).....	S5
S2.1. Synthesis of MUV-10 (Ca)	S5
S2.2. Time-resolved vs Static MUV-10	S9
<i>S2.2.1. Chemical Characterization.</i>	S9
X-Ray Diffraction Patterns (PXRD)	S9
Le Bail refinement.....	S9
Scanning Electron Microscopy (SEM-EDX).....	S10
Energy Dispersive X-Ray Analysis (EDX)	S11
Inductively Coupled Plasma with Mass Spectrometry (ICP-MS).....	S11
Thermogravimetric Analysis (TGA)	S12
N ₂ adsorption-desorption isotherms	S13
S2.3. Chemical Characterization: study of the crystal growth	S13
X-Ray Diffraction Patterns (PXRD)	S13
Scanning Electron Microscopy (SEM)	S14
Energy Dispersive X-Ray Analysis (EDX)	S15
N ₂ adsorption-desorption isotherms	S15
S3. Au@MUV-10	S16
S3.1. Synthesis of Au nanoparticles	S16
<i>S3.1.1. Chemical Characterization.</i>	S16
Ultraviolet-Visible Spectroscopy (UV-VIS)	S16
Dynamic Light Scattering (DLS)	S17
Transmission Electron Microscopy (TEM).....	S17
S3.2. Au@MUV-10 synthesis	S17
<i>S3.2.1. Chemical Characterization.</i>	S18
X-Ray Diffraction Patterns (PXRD)	S18
Le Bail refinement.....	S18
Scanning Electron Microscopy (SEM)	S19
Energy Dispersive X-Ray Analysis (EDX)	S19
Transmission Electron Microscopy (TEM).....	S20
Focused Ion Beam Scanning Electron Microscopy (FIB-SEM)	S21
Inductively Coupled Plasma with Mass Spectrometry (ICP-MS).....	S21

N ₂ adsorption-desorption isotherms	S22
S3.3. Higher gold loadings	S23
<i>S3.3.1. Chemical Characterization.</i>	S23
X-Ray Diffraction Patterns (PXRD)	S23
Scanning Electron Microscopy (SEM)	S24
Energy Dispersive X-Ray Analysis (EDX)	S24
Inductively Coupled Plasma with Mass Spectrometry (ICP-MS)	S25
N ₂ adsorption-desorption isotherms	S25
S4. Catalytic experiments	S26
S4.1. Cyclotrimerization of alkyne reaction	S26
<i>S4.1.1. Recyclability tests.</i>	S27
<i>S4.1.2. Kinetics and hot filtration studies</i>	S28
S4.2. Hydrochlorination of alkyne reaction.	S30
<i>S4.2.1. Recyclability tests.</i>	S30
<i>S4.2.2. Kinetics and hot filtration experiments</i>	S32
S5. References	S33

S1. General considerations: starting materials and characterization

Materials and reagents

Titanium (IV) isopropoxide (97%), anhydrous calcium chloride, acetic acid glacial (99.7%), tetrachloroauric (III) acid trihydrate (99%) and polyvinylpyrrolidone (≈ 40.000) were purchased from Sigma-Aldrich. Benzene-1,3,5-tricarboxylic acid (98%) was purchased from Alfa Aesar. *Tri*-sodium citrate tribasic dehydrate was purchased from Panreac. Methanol HPLC grade and *N,N*-dimethylformamide HPLC grade were purchased from Scharlau. All reagents and solvents purchased were used as received without further purification.

Structural and chemical characterization

- Time-resolved syntheses were carried out using a KD Scientific dual syringe pump Gemini 88 or additionally with an individual Legato 110 changing the infusion rate of addition.
- Powder X-Ray Diffraction (PXRD) patterns were collected in a PANalytical X'Pert Pro diffractometer using a copper radiation ($\text{Cu K}\alpha=1.5418 \text{ \AA}$) with an X'Celerator detector, operating at 40 mA and 45 Kv. Profiles were collected in the $2^\circ < 2\theta < 40^\circ$ range with a step size of 0.017° . XRD patterns for refinements were collected for polycrystalline samples using a 0.5 mm glass capillary mounted in the same equipment but using a Soller Slit of 0.02° and a divergence slit of $1/4^\circ$ at room temperature in the angular range $3^\circ < 2\theta < 40^\circ$ with a step size of 0.017° . LeBail refinements were carried out using the TOPAS software package.
- Scanning Electron microscopy and Energy-Dispersive X-Ray analysis (SEM-EDX): initial particle morphologies and dimensions were studied under a Hitachi S-4800 scanning electron microscope at an accelerating voltage of 20 kV, after treating the samples to a gold-palladium mixture metallization process during 90 seconds. Determination of the experimental metal ratio % (Ti and Ca) was determined with a Hitachi S-4800 EDX analysis for the different solids.
- Transmission Electron microscopy (TEM): high resolution morphology images of the material were obtained with a Hitachi HT-7800 transmission electron microscope at an accelerating voltage of 100 kV, after preparing the samples in aluminium mesh grids from TED PELLA, INC.
- Focused Ion Beam Scanning Electron Microscope (FIB-SEM): spatial distribution of the nanoparticles inside the materials was studied under a Thermo Fisher Scientific Scios 2 DualBeam (FESEM) by cross-section analysis using the ion beam at an accelerated voltage of 30Kv. Pt protective layer was deposited at a current of 0.5nA, followed by the dissection at 15nA and the final polish step at 3nA. SEM images were taken with the electron beam at an accelerating voltage of 3kV and a current of 0.2nA.
- Analysis of N_2 adsorption-desorption isotherms at 77 K: gas adsorption/desorption measurements were recorded on a Micromeritics 3Flex apparatus at relative pressures up to 1 atm. Prior to analysis, samples were washed by soxhlet in MeOH overnight and then degassed overnight at 120°C and 10^{-6} Torr. Surface area, pore size and volume values were calculated from N_2 adsorption-desorption isotherms (77 K). Specific surface areas were calculated by multi-point Brunauer-Emmet-Teller (BET) method recommended for microporous materials. Total pore volume values were taken at $P/P_0=0.95$. Pore size distributions were analysed by the solid density functional theory (NLDFT) for the adsorption branch by assuming a cylindrical pore model.

- Inductively Coupled Plasma with Mass Spectrometry (ICP-MS): gold content in the materials was determined by trace analysis using an Agilent ICPMS7900.
- Ultraviolet-Visible Spectroscopy (UV-VIS): gold nanoparticle concentration and size were recorded by UV-VIS absorption spectra on a Jasco V-670 spectrophotometer in a baseline from 300 to 800 nm range, using 10.00 mm optical path quartz glass standard cuvettes.
- Thermogravimetric Analysis (TGA) was carried out with a Waters/TA Instruments TGA550 apparatus between 25 and 700 °C under ambient conditions (5 °C·min⁻¹ scan rate and an air flow of 30 mL·min⁻¹). Samples were mounted on a 25-position autosampler.
- Dynamic Light Scattering (DLS) nanoparticle analysis: gold nanoparticle size and polydispersion was recorded with a Zetasizer Nano ZS Instrument (Malvern Instruments Ltd.) at room temperature in order to measure the dynamic diameter of the gold nanoparticles in solution, providing information on the aggregation state of the nanoparticles in solution.
- Gas Chromatography with Flame Ionisation Detector (GC-FID): was used to examine the course of the catalytic reactions. The equipment was an Agilent 6980N with a column installed of the following characteristics: Agilent 199091 J-413 HP-5 with the following dimensions: 30 m x 320 µm x 0.25 µm.

S2. Time-resolved Synthesis of MUV-10 (Ca)

S2.1. Synthesis of MUV-10 (Ca)

Following the synthetic conditions previously reported for MUV-10 by Castells et al.¹ 325.9 mg of benzene-1,3,5-tricarboxylic acid (H₃btc, 1.54 mmol) were dissolved in 20 ml of *N,N*-dimethylformamide (259.6 mmol) in a 20 ml BD plastic syringe. Another solution was prepared for a different 20ml plastic syringe consisting on 34.6 mg of CaCl₂ anhydrous (311 µmol) and 92.4 µl of Ti(OⁱPr₄) (312 µmol) in 11.2 ml of *N,N*-dimethylformamide (144.7 mmol) and 8.9 ml of acetic acid glacial (155.5 mmol). The two solutions were controllably added separately to the time-resolved synthetic setup which was already preheated at 120 °C and under inert atmosphere conditions. The addition speed was slowed throughout the synthetic addition and let to react for 24 hours. After cooling down to room temperature, the white powder was recovered by centrifugation and washed thoroughly with fresh DMF (4 x 30 ml) and methanol (2 x 30 ml). The solid was further washed by Soxhlet extraction with methanol overnight and dried at room temperature prior to characterisation.

Table S1. Optimal addition rate of reaction

	Addition rate (ml·h ⁻¹)	Metal volume added (mL)	Ligand volume added (mL)	[Metal] (mM)	[Ligand] (mM)	Time (hours)
t ₁	20	3.38	3.38	7.7	38.12	0.17
t ₂	12	3.38	3.38	7.7	38.12	0.45
t ₃	10	3.38	3.38	7.7	38.12	0.79
t ₄	8	3.38	3.38	7.7	38.12	1.21
t ₅	6	3.38	3.38	7.7	38.12	1.78
t ₆	-	-	-	-	-	24

Before the optimal addition rate parameters were obtained several trial and error experiments were carried out under the following conditions below Table S2 to S4. Different addition rates and different volumes were added to the reactor were polycrystallization or loss of homogeneity was obtained.

Table S2. Faster addition rate over 5 hours

Addition rate (ml·h ⁻¹)	Volume added (mL)	[Metal] (mM)	[L](mM)	Time (hours)
40	20.4	7.65	37.93	0.26
20	40.8	7.65	37.93	0.77
10	61.2	7.65	37.93	1.79
8	81.6	7.65	37.93	3.06
6	102	7.65	37.93	4.76

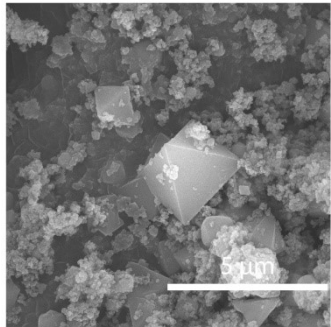
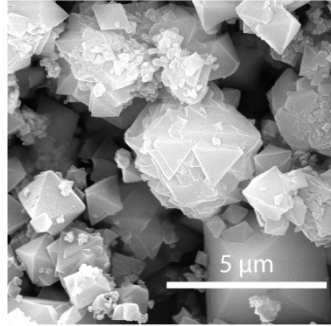


Table S3. Faster addition rate prolonged over 13.5 hours

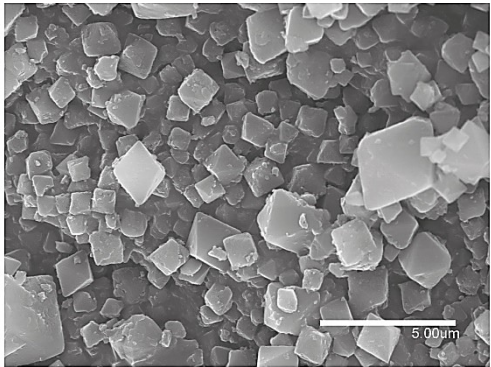
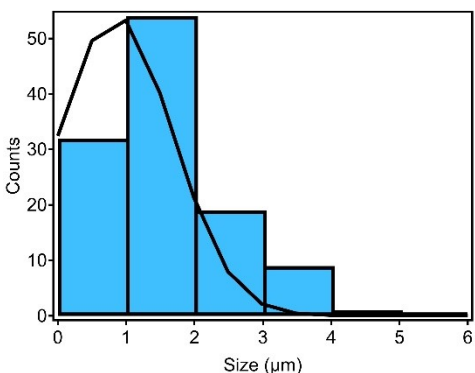
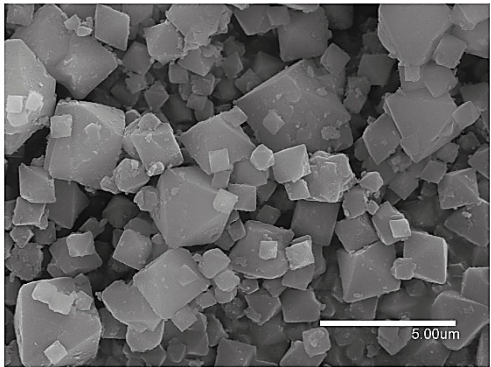
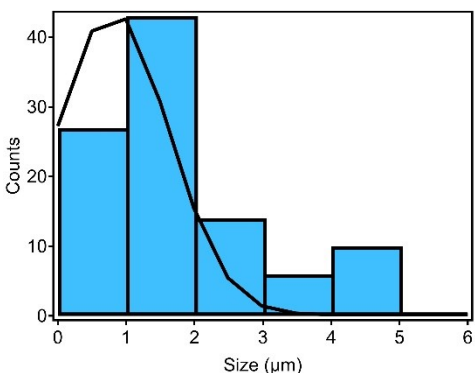
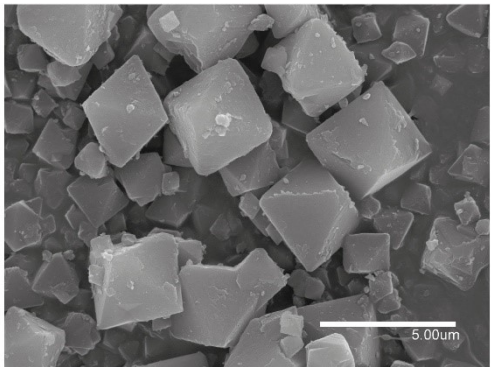
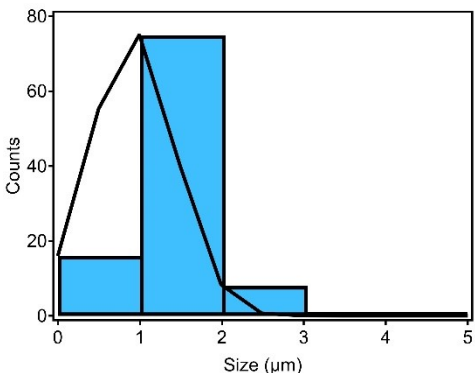
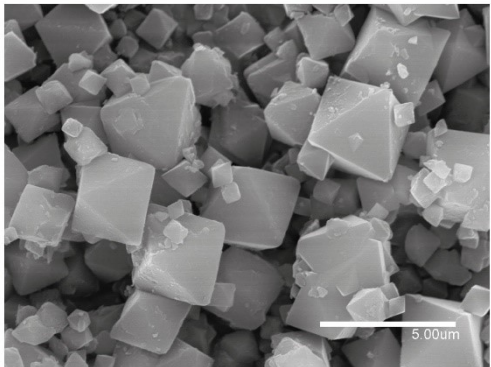
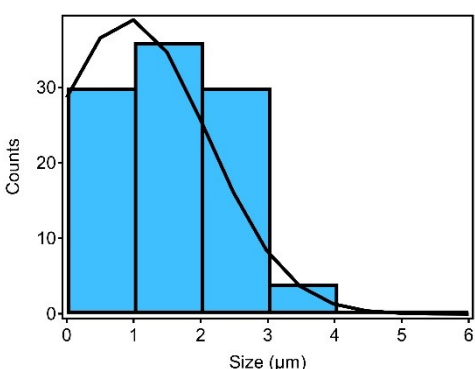
Addition rate (ml·h ⁻¹)	Volume added (mL)	[Metal] (mM)	[L](mM)	Time (hours)
50	20.40	24.47	121.33	0.20
25	40.80	24.47	121.33	0.61
20	51.00	24.47	121.33	1.12
17.5	58.30	24.47	121.33	1.70
15	68.00	24.47	121.33	2.38
12.5	81.59	24.47	121.33	3.20
10	10.20	24.47	121.33	4.22
6	17.00	24.47	121.33	5.92
4	25.50	24.47	121.33	8.47
2	51.00	24.47	121.33	13.50

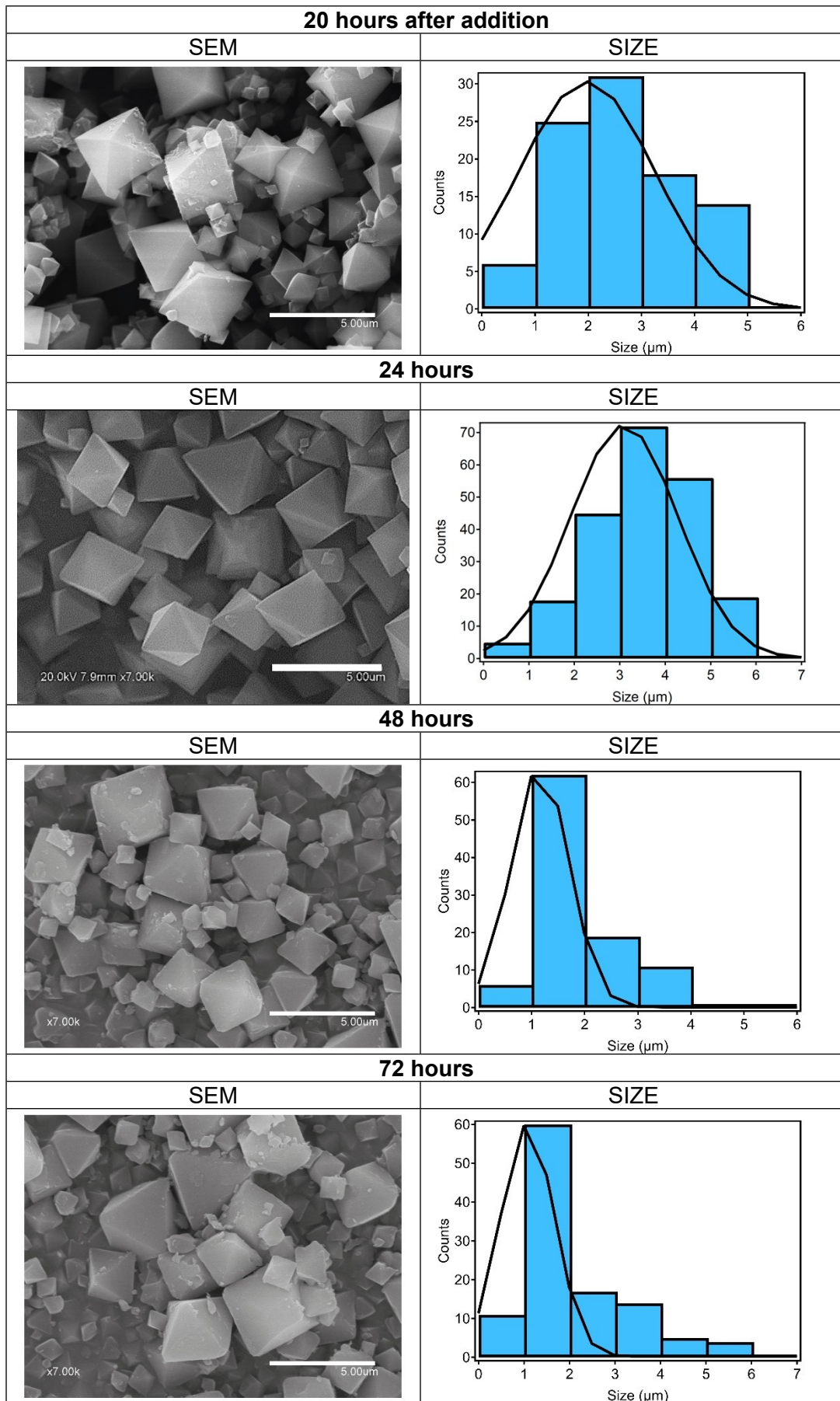


Scale-up: MUV-10 time-resolved could be synthesized at gram scale following the same procedure described above by adding 845.6 mg of benzene-1,3,5-tricarboxylic acid (H₃btc, 4.02 mmol) dissolved in 53 ml of *N,N*-dimethylformamide (684.53 mmol) in a 50 ml BD plastic syringe and another solution consisting on 90 mg of CaCl₂ anhydrous (811 μmol) and 240 μl of Ti(OⁱPr₄) (810 μmol) in 29 ml of *N,N*-dimethylformamide (374.55 mmol) and 24 ml of acetic acid glacial (419.25 mmol), therefore demonstrating that this synthetic methodology can be applied to bigger reactors such as industrial procedures.

Furthermore, reaction time is also optimised as aliquots were taken at 2, 4, 8, 16, 20, 24, 48 and 72 hours. It was observed by Scanning Electron Microscopy (SEM) that crystals' size reached plateau at 24 hours as it is observed that homogeneity is lost at 48 hours and times shorter than 24 crystals size varies in a wide range. All this information has been collected in table S4.

Table S4. Time reaction optimization.

2 hours after addition	
SEM	SIZE
	
4 hours after addition	
SEM	SIZE
	
8 hours after addition	
SEM	SIZE
	
16 hours after addition	
SEM	SIZE
	



S2.2. Time-resolved vs Static MUV-10

In order to determine if the *de novo* synthetic methodology was successful the same chemical characterisation techniques as previously reported for MUV-10 (Ca)¹ were performed.

S2.2.1. Chemical Characterization.

X-Ray Diffraction Patterns (PXRD)

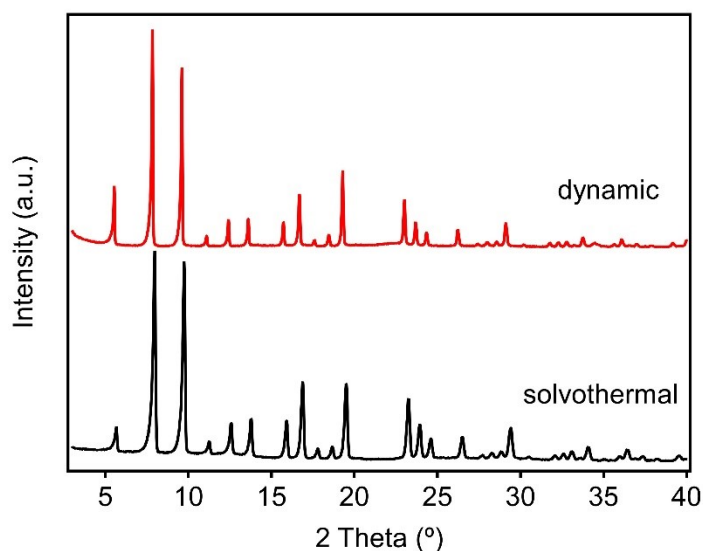
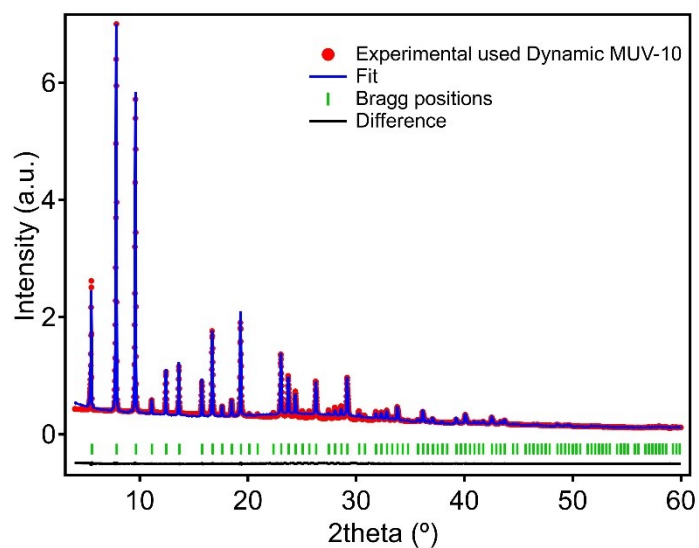


Figure S1. Comparison of the PXRD of Time-resolved and Solvothermal MUV-10.

Le Bail refinement

Le Bail refinements were carried out with the TOPAS software package using MUV-10 (Ca) previously reported parameters of MUV-10¹. The refined cell parameters obtained for MUV-10 time-resolved are the following: Pm-3, $a=b=c= 15.88924 \text{ \AA}$; $\alpha=\beta=\gamma= 90^\circ$, $R_p= 6.08\%$, $R_{wp}=7.80\%$, $R_{exp}= 2.06\%$, $\chi^2=0.0001$, $GoF=3.78$. The agreement between the experimental and the predicted diffractogram of MUV-10 (Ca) discards any changes in the structure and confirms the similarity among the two synthetic procedures.

a)



b)

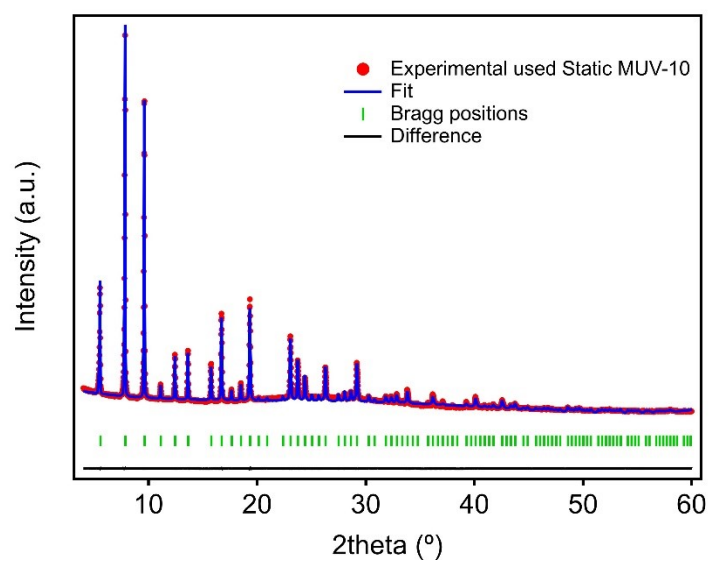


Figure S2. Comparison of the Le Bail refinements of (a) Time-resolved MUV-10 and (b) Static MUV-10.

Scanning Electron Microscopy (SEM-EDX)

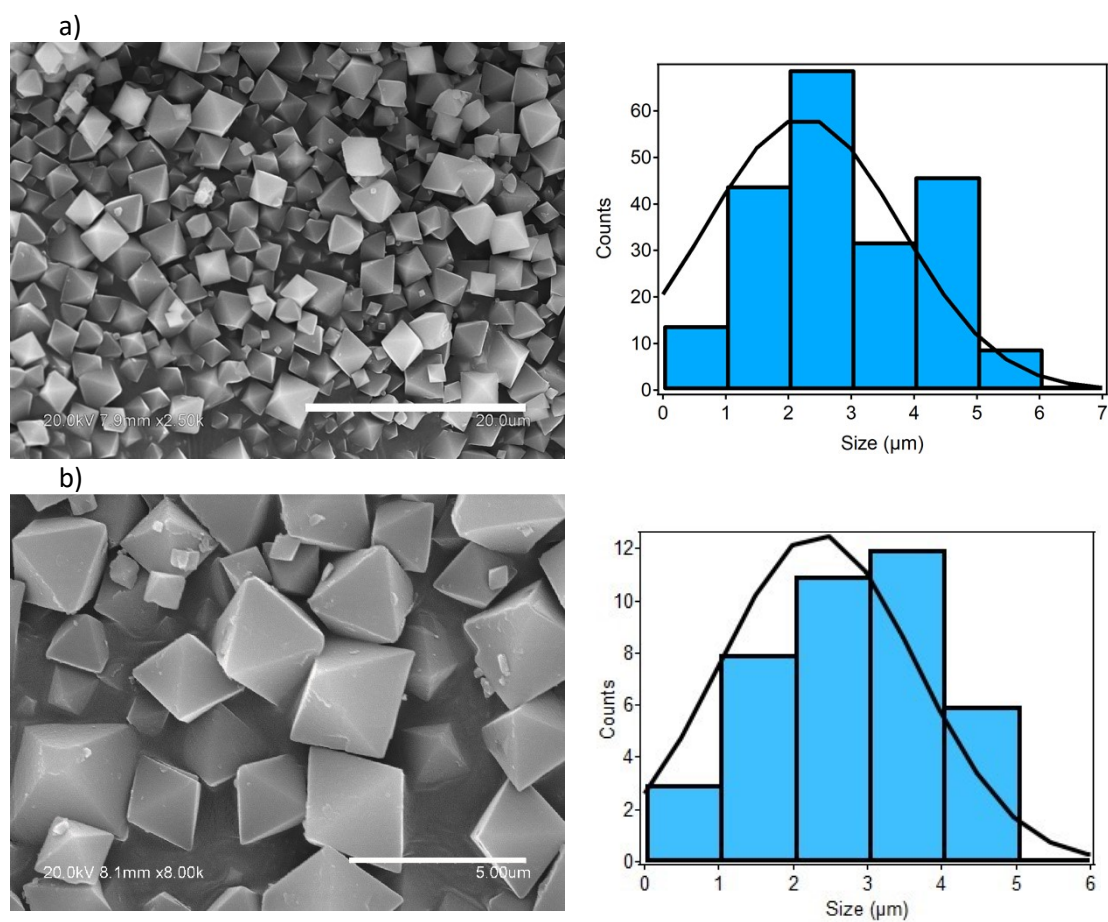


Figure S3. On the right SEM images and on the left size histogram calculated from them on the stages: a) Time-resolved MUV-10 and b) Static MUV-10.

Energy Dispersive X-Ray Analysis (EDX)

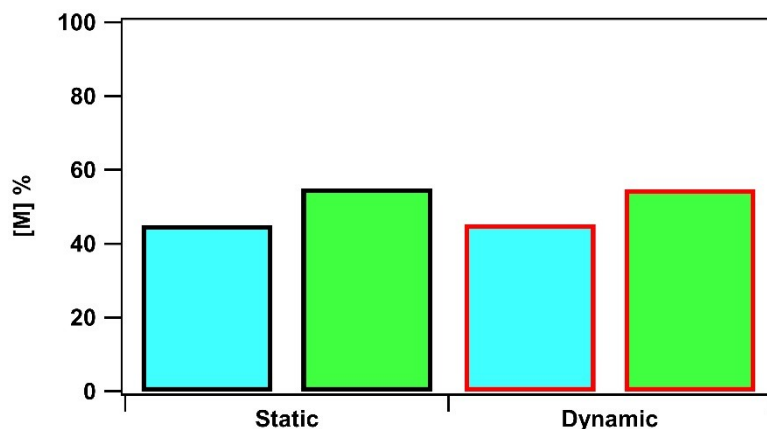


Figure S4. Experimental Ti:Ca ratio from point and shoot EDX analysis.

Inductively Coupled Plasma with Mass Spectrometry (ICP-MS)

Table S5. Total metal content determined by ICP-MS.

	Ca (%)	Ti (%)
Static MUV-10 (Ca)	48.7	51.3
Time-resolved MUV-10 (Ca)	48.2	51.8

Thermogravimetric Analysis (TGA)

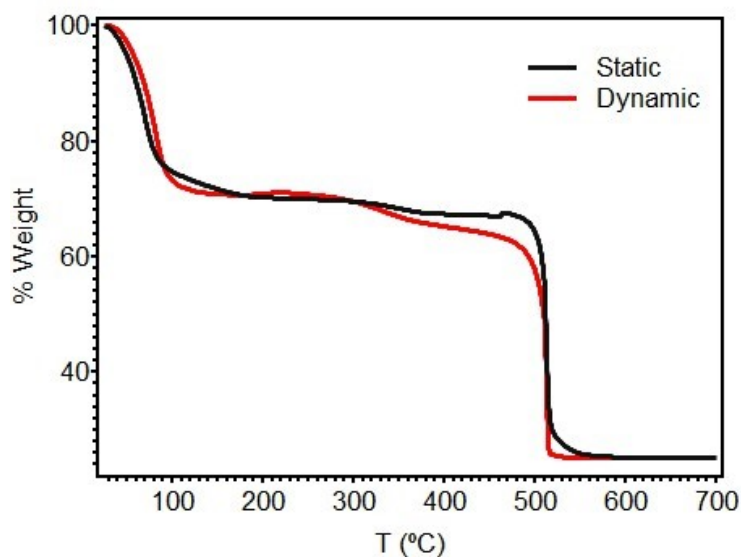


Figure S5. Thermal decomposition profile of MUV-10 by time-resolved synthesis and by solvothermal synthesis.

N₂ adsorption-desorption isotherms

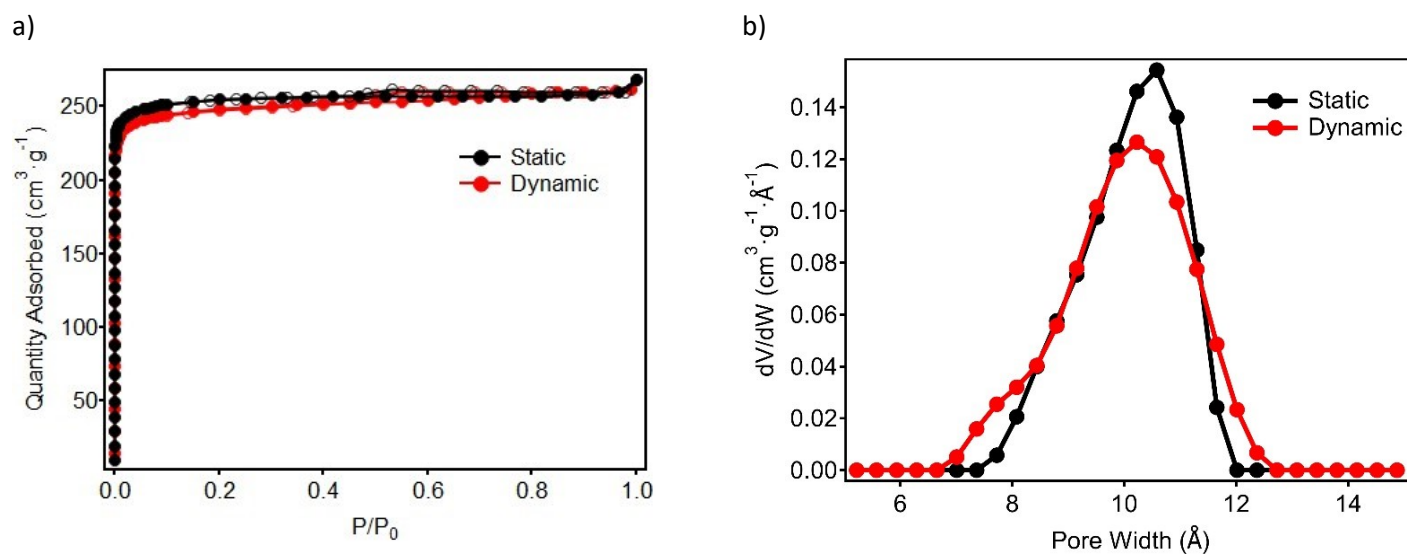


Figure S6. a) N₂ Adsorption-desorption isotherms at 77 K and b) Pore size distribution calculated assuming a cylindrical pore model during the time-resolved synthesis.

Table S6. Summary of the N₂ adsorption isotherms at 77 K.

	BET Surface area (m ² ·g ⁻¹)	Total Pore Volume (cm ³ ·g ⁻¹)
Static	1042.1 ± 0.2	0.4
Time-resolved	1007.6 ± 0.9	0.4

S2.3. Chemical Characterization: study of the crystal growth

The crystal growth evolution throughout the addition synthetic process was studied and fully characterised as in the previous section S2.2.

X-Ray Diffraction Patterns (PXRD)

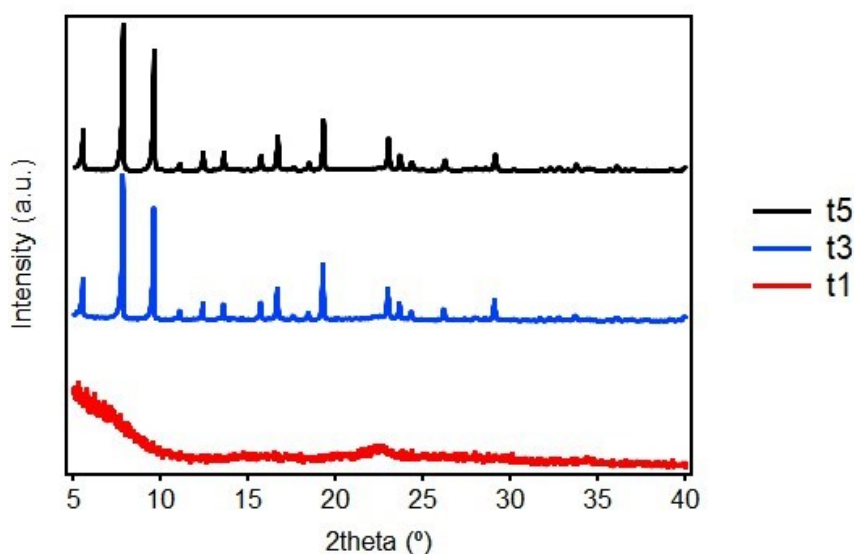
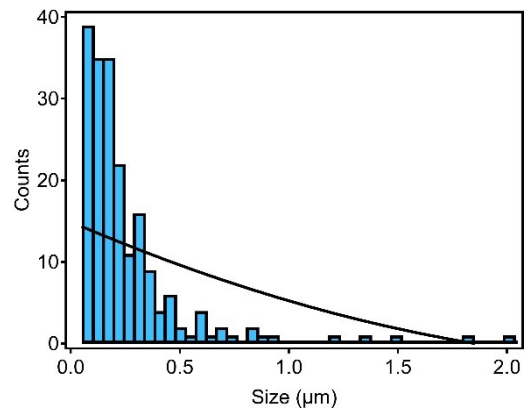
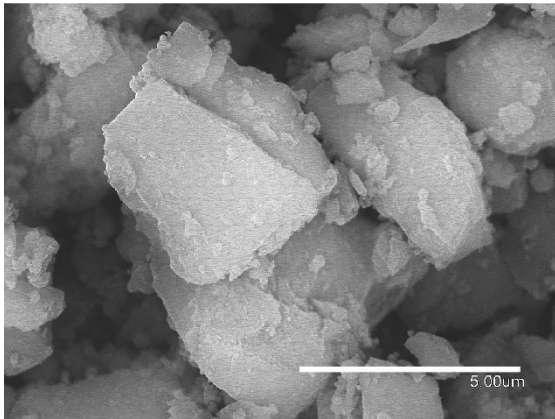


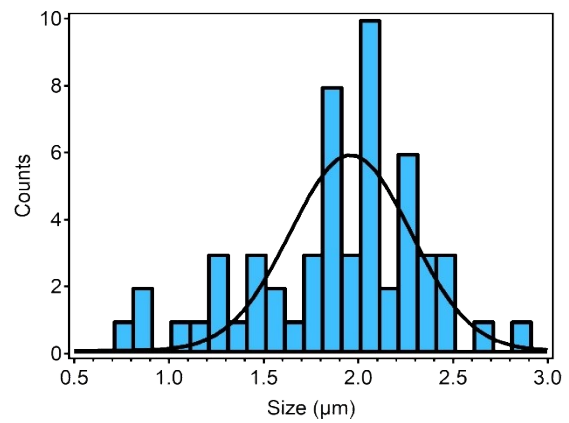
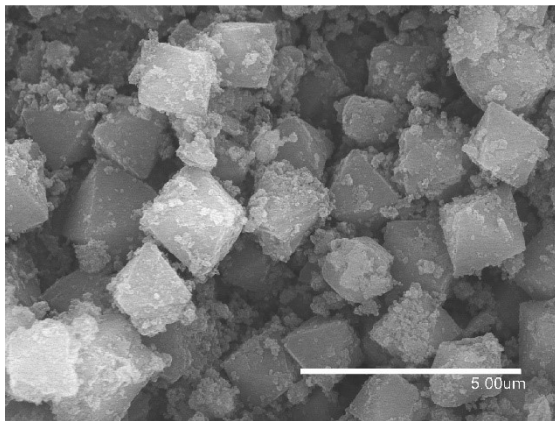
Figure S7. Comparison of the PXRD in the different stages of the time-resolved reaction of MUV-10.

Scanning Electron Microscopy (SEM)

a)



b)



c)

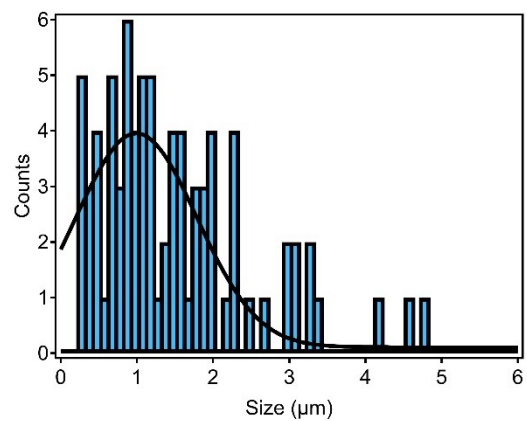
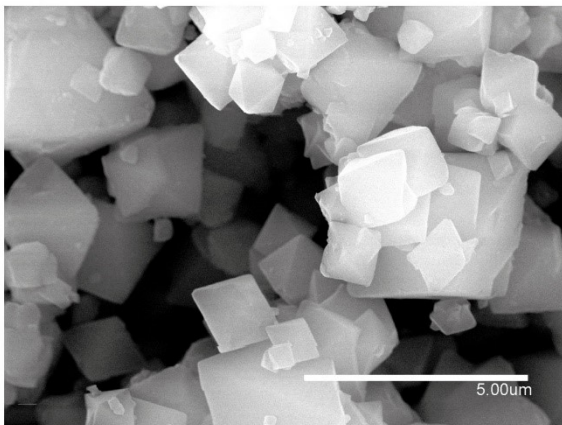


Figure S8. On the right SEM images and on the left size histogram calculated from them on the stages: a) t1; b) t3 and c) t5.

Energy Dispersive X-Ray Analysis (EDX)

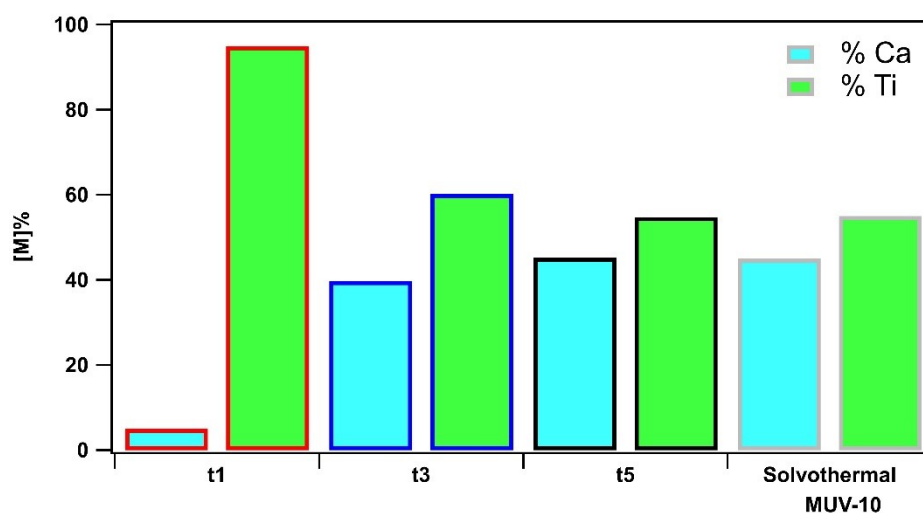


Figure S9. Incorporation study of the calcium: titanium ratio of the material during the synthetic process acquired by SEM-EDX.

N₂ adsorption-desorption isotherms

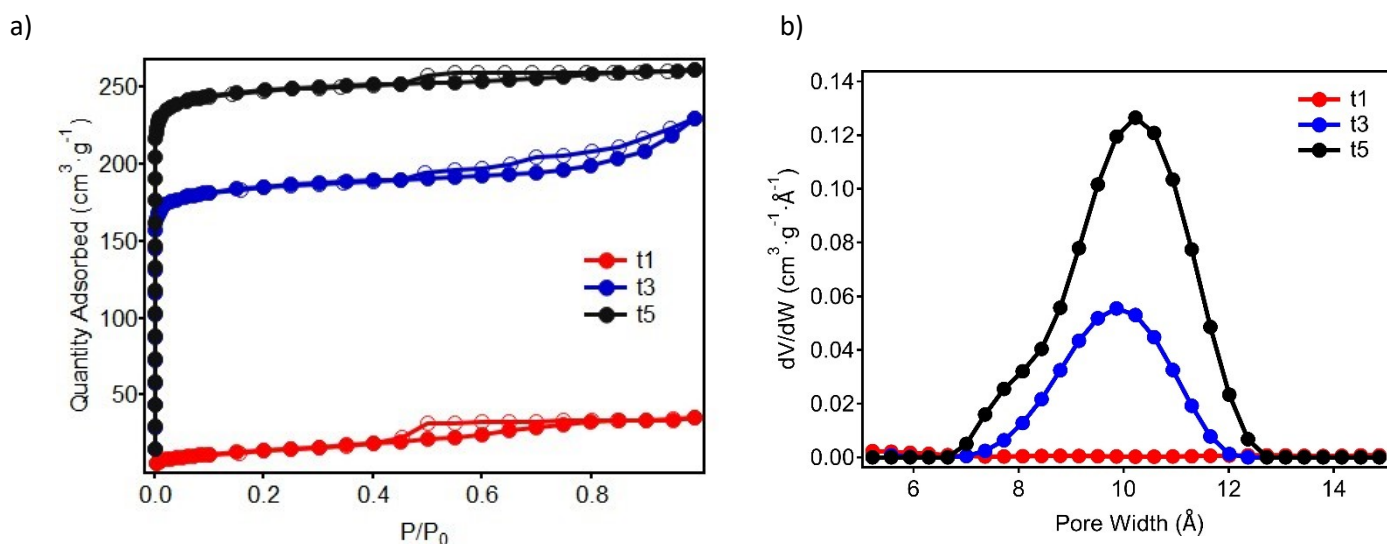


Figure S10. a) N₂ Adsorption-desorption isotherms at 77 K and b) Pore size distribution calculated assuming a cylindrical pore model during the time-resolved synthesis.

Table S7. Summary of the N₂ adsorption isotherms at 77 K.

	BET Surface area (m ² ·g ⁻¹)	Total Pore Volume (cm ³ ·g ⁻¹)
t1	50.9 ± 0.1	0.05
t3	441.2 ± 0.8	0.2
t5	1002.8 ± 0.7	0.4

S3. Au@MUV-10

S3.1. Synthesis of Au nanoparticles

Gold nanoparticles spheres were prepared following the reported Turkevich's ² reduction methodology prior to their injection in the time-resolved synthesis. Firstly, 4.5 ml of an aqueous sodium citrate solution (1%) were dropped in a boiling an aqueous solution of HAuCl₄·3H₂O (0.01%, 150 mL) in a round bottom flash fitted with a reflux condenser under stirring. The boiling mixture was let to react for 20 minutes. The resulting dark red solution is removed from heat and cooled down in a water ice bath setup until room temperature is reached. Afterwards, an aqueous solution of PVP (500 mg, Mw ≈ 55.000) is added dropwise to the Au mixture under stirring. The final solution was left at room temperature under stirring for 24 hours.

The PVP-stabilized gold sphere NPs were collected by centrifugation at 13.000 rpm for 30 minutes and 4 °C and then washed with fresh methanol (3x30 mL). The final red precipitate was redispersed in methanol for further characterization.

S3.1.1. Chemical Characterization.

Ultraviolet-Visible Spectroscopy (UV-VIS)

Concentration of gold nanoparticles in solution is estimated by reported calculations³ by taking the absorbance value of the solution at 400 nm.

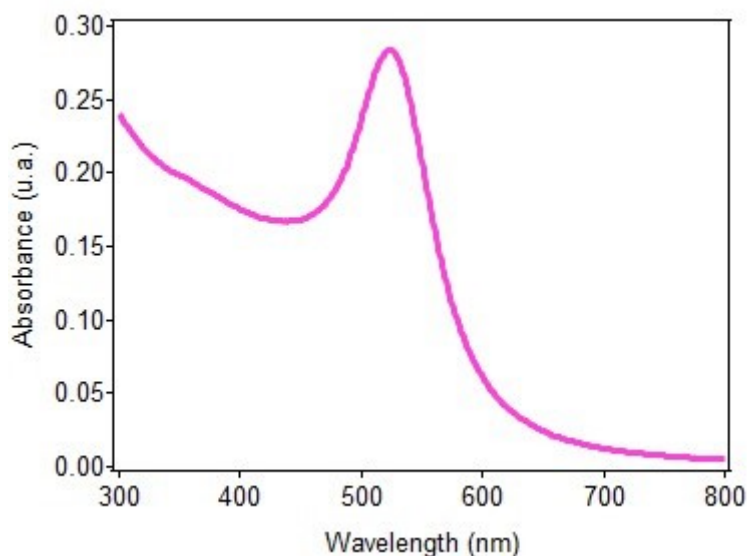


Figure S11. UV-Vis spectrum for the spherical Au NPs with a maximum absorbance at ~520 nm indicating a 20 nm size.

Dynamic Light Scattering (DLS)

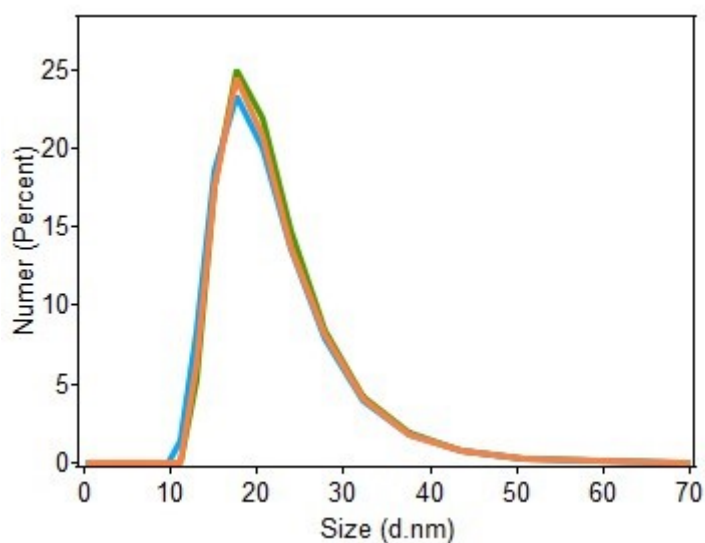


Figure S12. Size dispersion spectrum for the 20 nm size spherical gold nanoparticles.

Transmission Electron Microscopy (TEM)

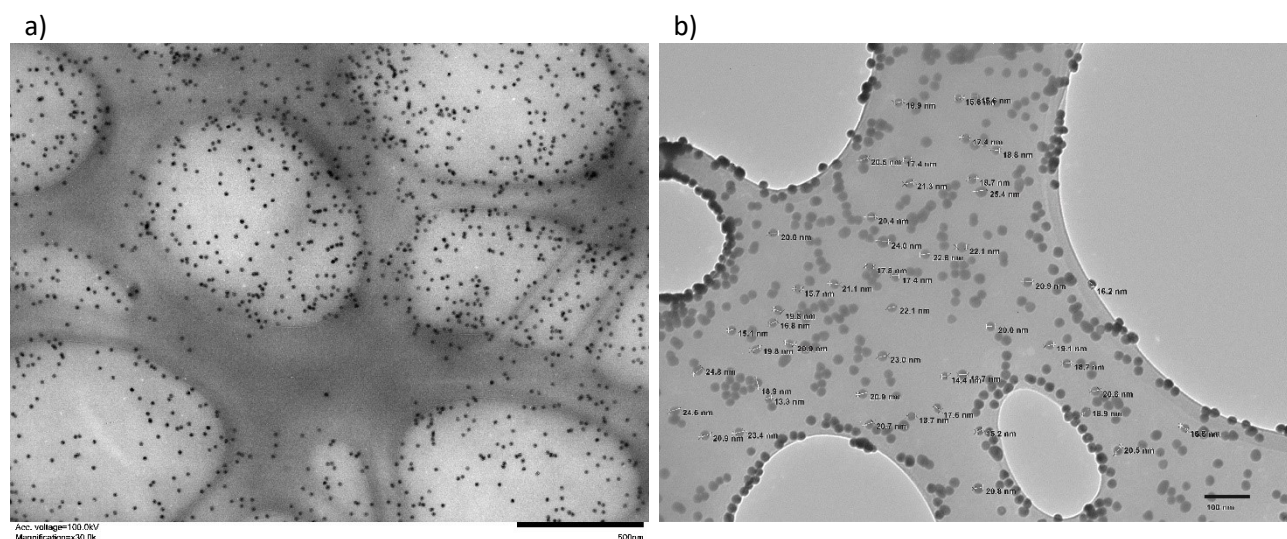


Figure S13. a) TEM images of the gold nanoparticles visually b) confirming the 15-20 nm size.

S3.2. Au@MUV-10 synthesis

Following the time-resolved procedure, 1 ml of the pre-synthesised Au NPs (0.035mM) were injected into the reactor during the time-resolved synthesis at three different: *amorphous* (t=0 mins.), *incipient* (t=27 mins.) and *fully formed* (t=105 mins.). All samples were left to react for 24 hours at 120 °C under inert atmosphere. After cooling down to room temperature, the pink powder precipitate was recovered by centrifugation and rinsed with fresh DMF (4 x 30 ml) and methanol (2 x 30 ml). The obtained solid was further washed by Soxhlet extraction with methanol for three cycles and dried at room temperature prior to further characterization.

S3.2.1. Chemical Characterization.

X-Ray Diffraction Patterns (PXRD)

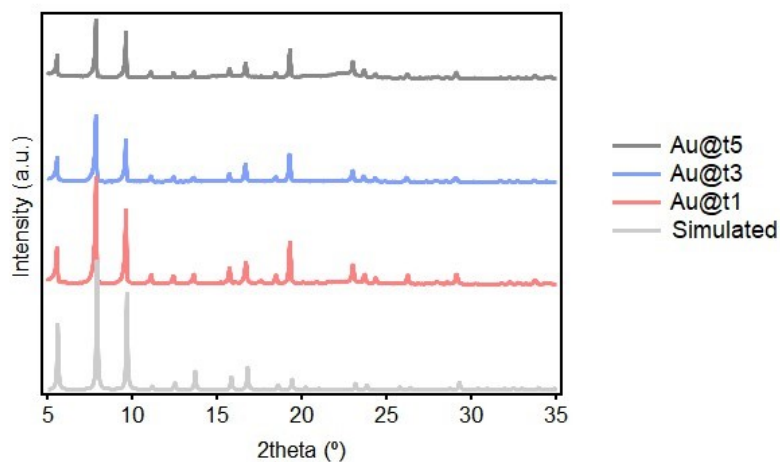


Figure S14. Comparison of the PXRD of the different Au@MUV-10 samples compared to solvothermal MUV-10.

Le Bail refinement

Le Bail refinements were carried out with the TOPAS software package using MUV-10 (Ca) previously reported parameters of MUV-10¹. The refined cell parameters obtained are the following: Pm-3, $a=b=c= 15.89481 \text{ \AA}$; $\alpha=\beta=\gamma= 90^\circ$, $R_p= 4.78\%$, $R_{wp}=6.19\%$, $R_{exp}= 2.48\%$, $\chi^2=0.0001$, $GoF=2.50$. The agreement between the experimental and the predicted diffractogram of MUV-10 (Ca) discards any changes in the structure and confirms the similarity among the two synthetic procedures.

a) Au@t1

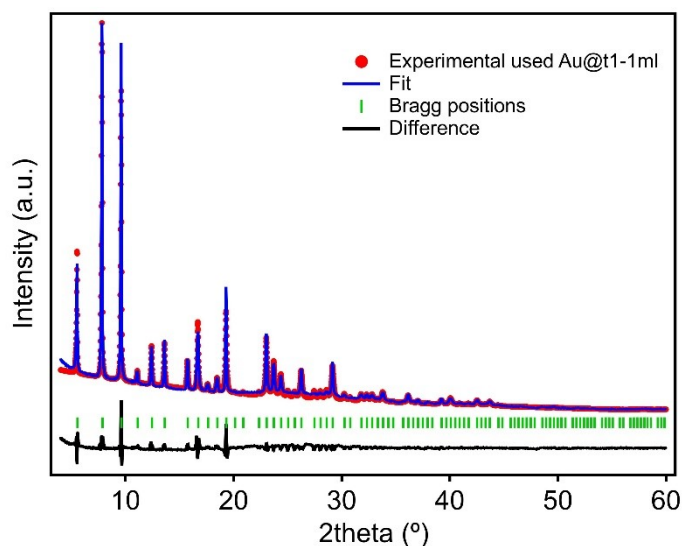


Figure S15. Le Bail refinements of Au@t1

Scanning Electron Microscopy (SEM)

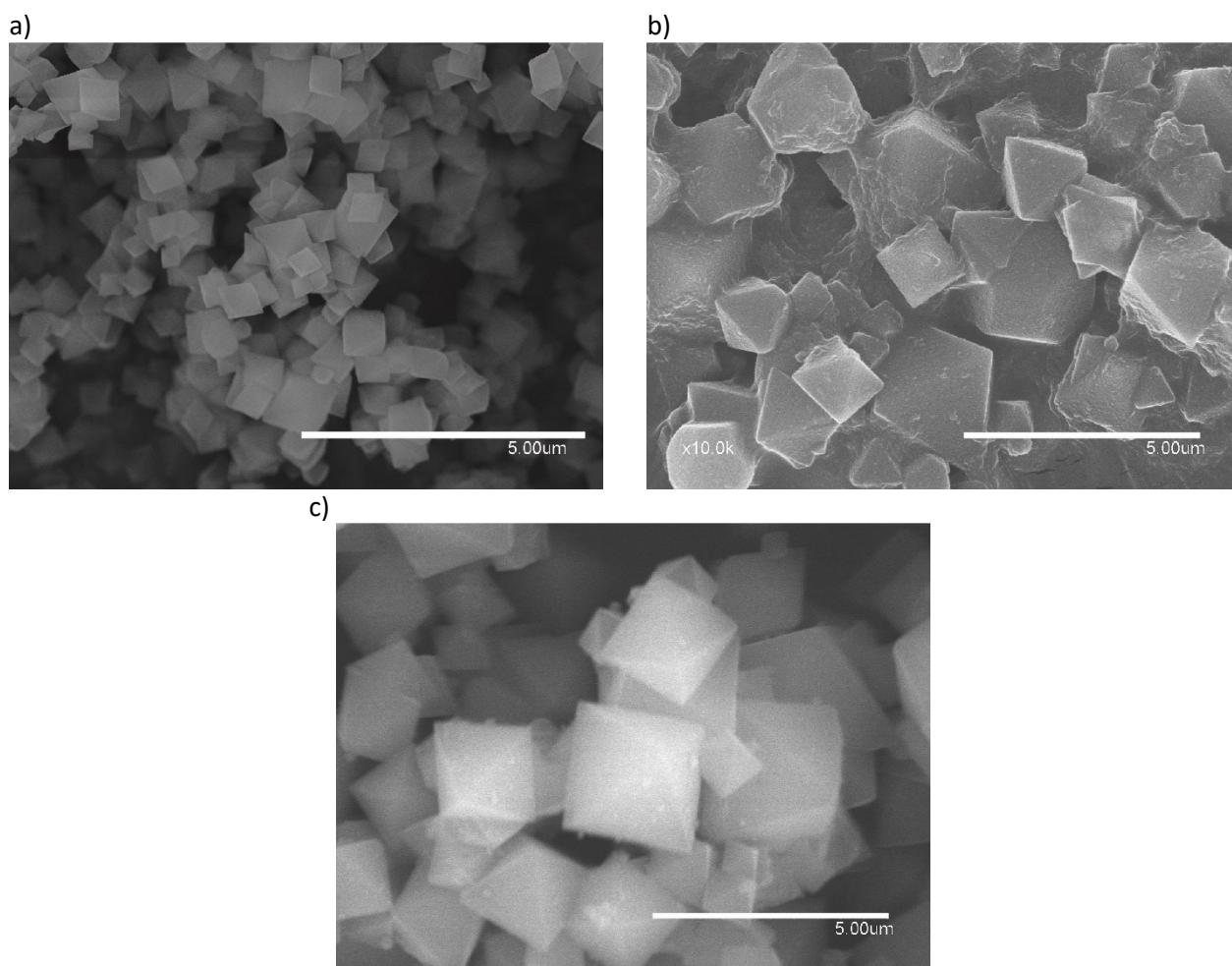


Figure S16. SEM images of the different Au@MUV-10 samples a) Au@t1, b) Au@t3 and Au@t5.

Energy Dispersive X-Ray Analysis (EDX)

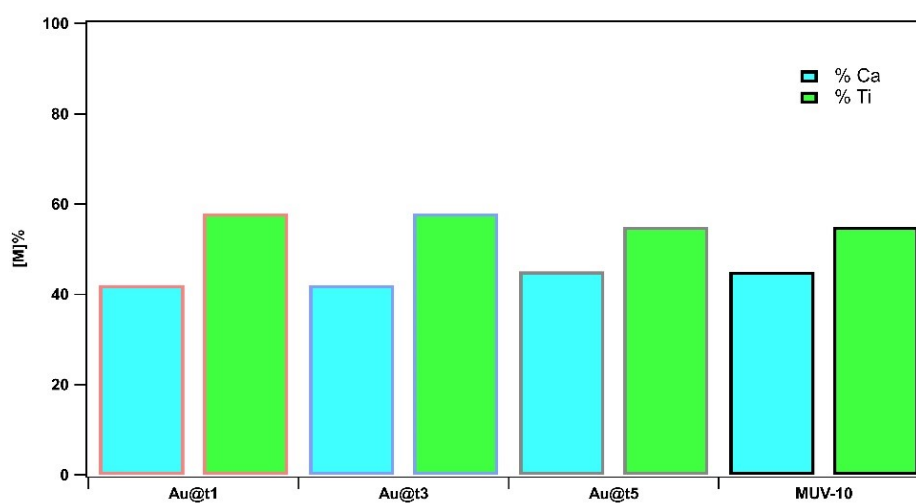


Figure S17. Experimental Ti:Ca ratio % from EDX analysis of each sample.

Transmission Electron Microscopy (TEM)

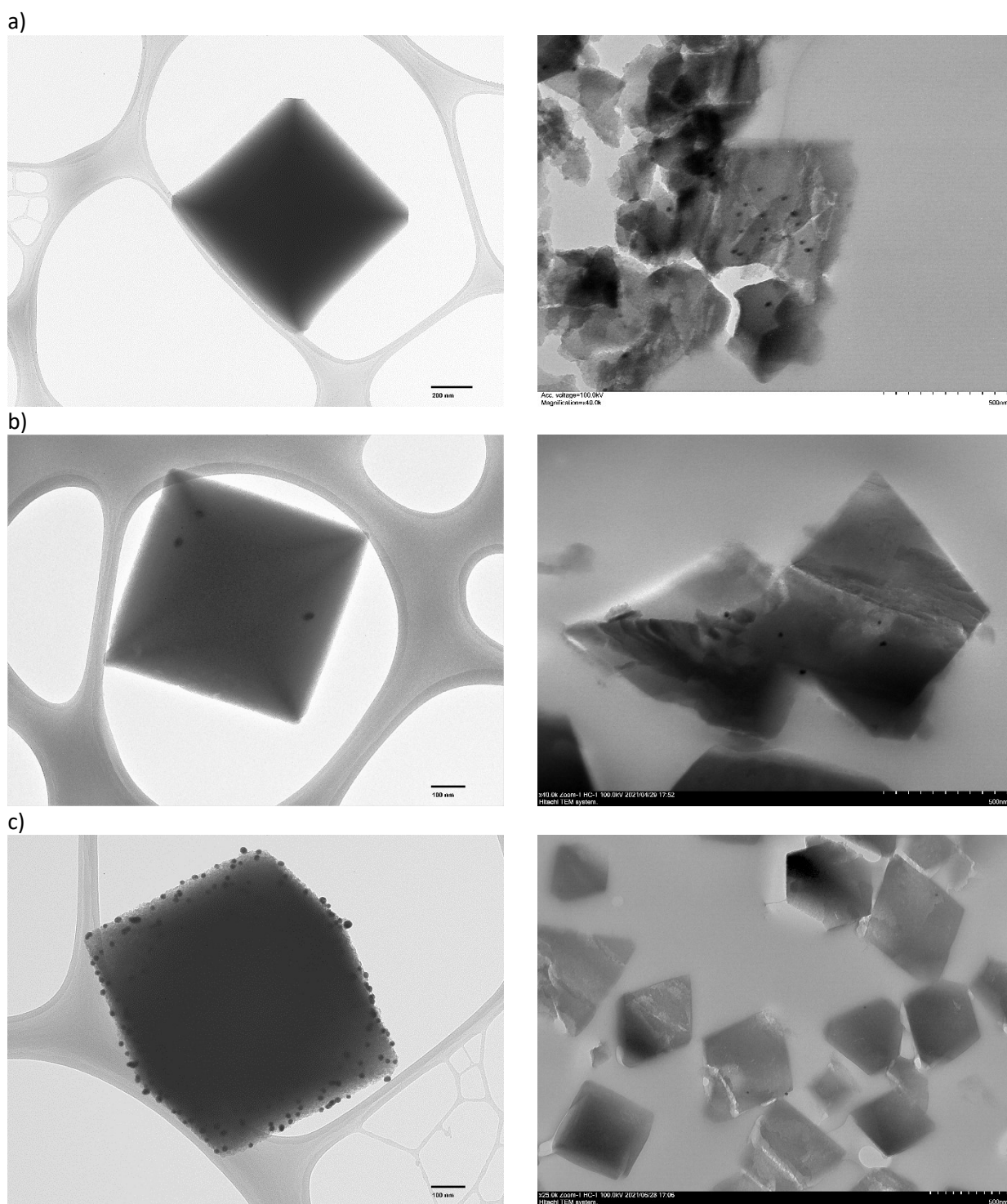


Figure S18. TEM images of the different Au@MUV-10 samples on the right a picture of the Au@MUV-10 and on the left a laser-cut view of the crystal for a) Au@t1, b) Au@t3 and c) Au@t5 (without Soxhlet washing).

Focused Ion Beam Scanning Electron Microscopy (FIB-SEM)

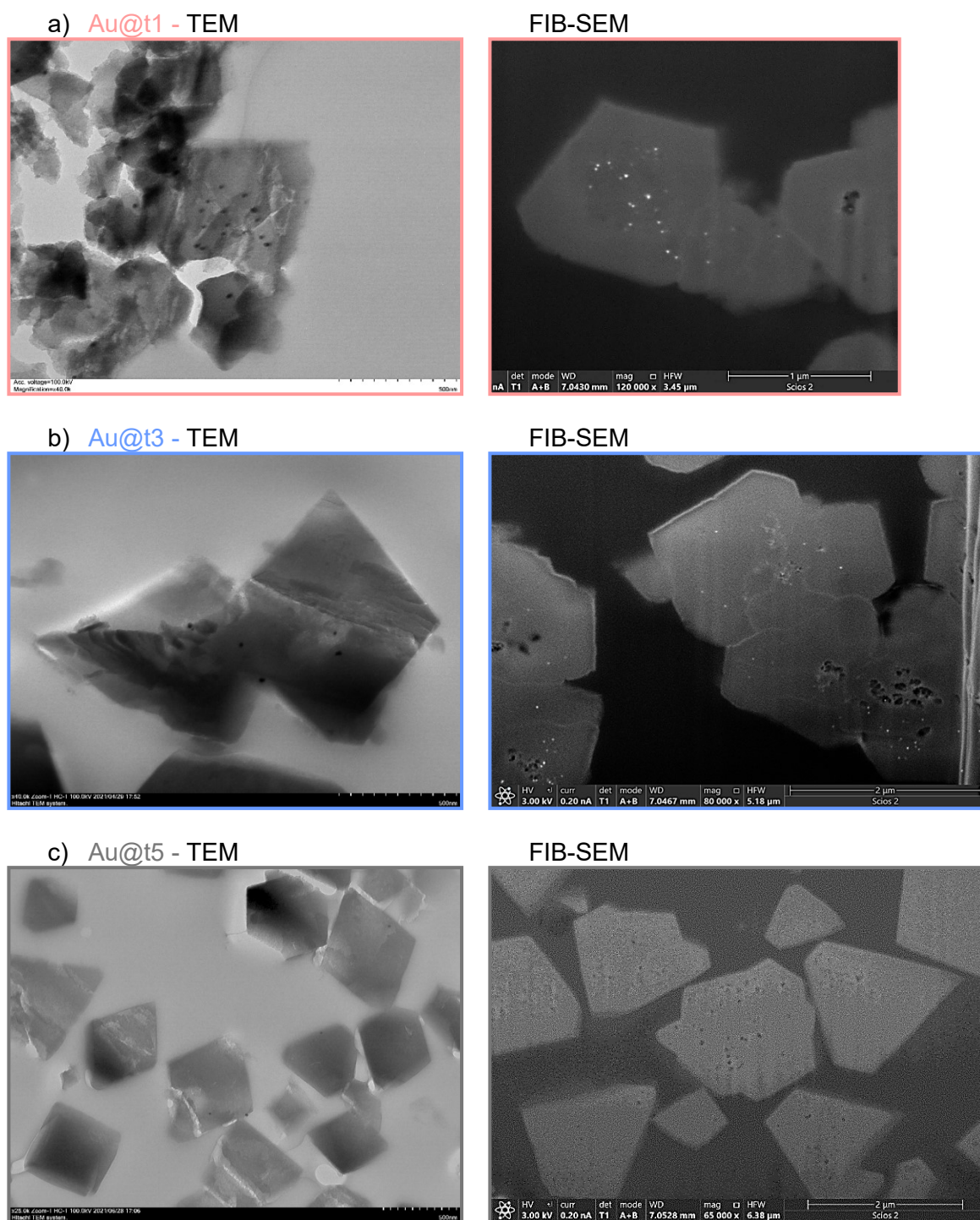


Figure S19. TEM and FIB-SEM images of the different Au@MUV-10 samples on the right a laser-cut view of the crystals and on the left FIB-SEM images of the same samples for a) Au@t1, c) Au@t3 and c) Au@t5.

Inductively Coupled Plasma with Mass Spectrometry (ICP-MS)

Table S8. ICP-MS data with the amount of gold incorporated in the materials adding 1 ml of the desired concentration.

	Au (mg/Kg)
Au@t1	187.0 ± 4
Au@t3	243 ± 3
Au@t5	160.7 ± 0.8

N₂ adsorption-desorption isotherms

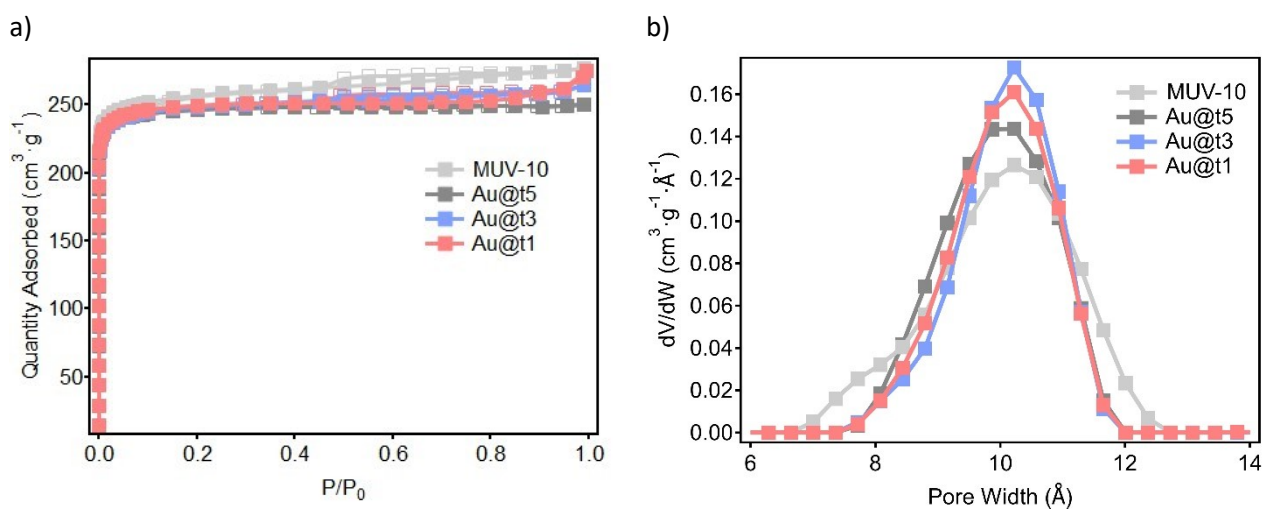


Figure S20. a) N₂ Adsorption-desorption isotherms at 77 K and b) Pore size distribution calculated assuming a cylindrical pore model during the time-resolved synthesis.

Table S9. Summary of the N₂ adsorption isotherms at 77 K.

	BET Surface area (m ² ·g ⁻¹)	Total Pore Volume (cm ³ ·g ⁻¹)
Au@t1	1014.4 ± 0.6	0.4
Au@t3	1005.7 ± 0.5	0.4
Au@t5	1005.9 ± 0.6	0.4
MUV-10 (Ca)	1041.2 ± 0.2	0.4

S3.3. Higher gold loadings

Once the integration of the nanoparticles inside the MUV-10 was demonstrated, a higher volume (5 ml and 10 ml) of 20 nm gold nanoparticles was injected at the same speed ($20 \text{ ml}\cdot\text{h}^{-1}$) in Au@t1 in order to further study the gold incorporation and their catalytical properties (see section S4). The synthetic procedure is the same as in Au@MUV-10 (see section 3.3). Therefore 3 new samples were obtained Au@t1 – 1ml, Au@t1 – 5ml and Au@t1 – 10ml.

S3.3.1. Chemical Characterization.

X-Ray Diffraction Patterns (PXRD)

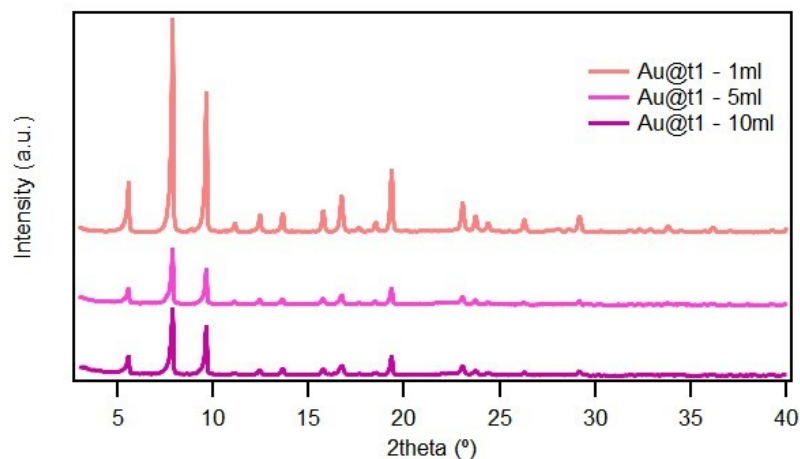


Figure S21. Comparison of the PXRD of the different Au@t1 samples with the different loadings of gold.

Scanning Electron Microscopy (SEM)

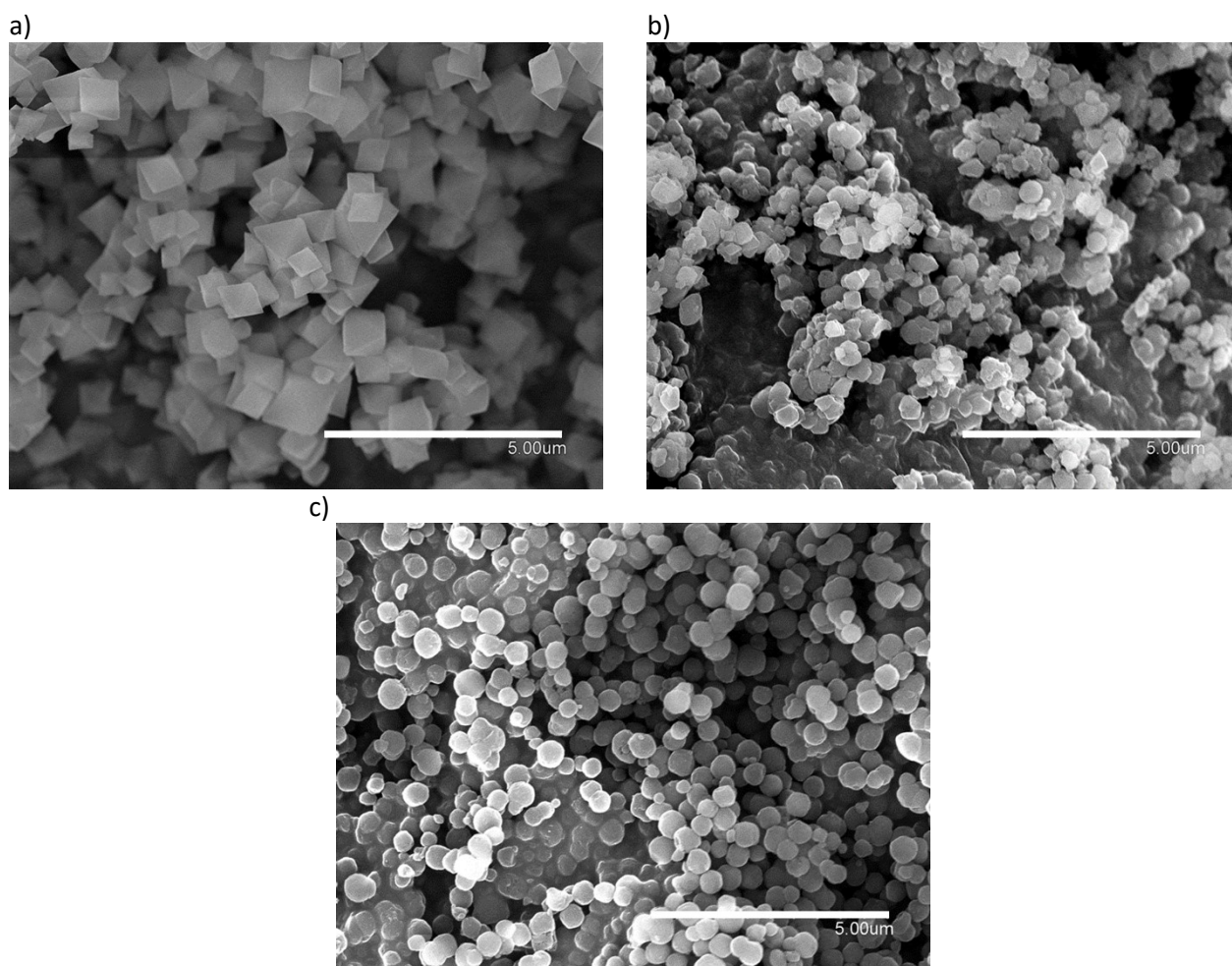


Figure S22. SEM images of the different Au@MUV-10 samples a) Au@t1-1ml, b) Au@t-5ml and Au@t1-10ml. All images were taken at the same focal distance.

Energy Dispersive X-Ray Analysis (EDX)

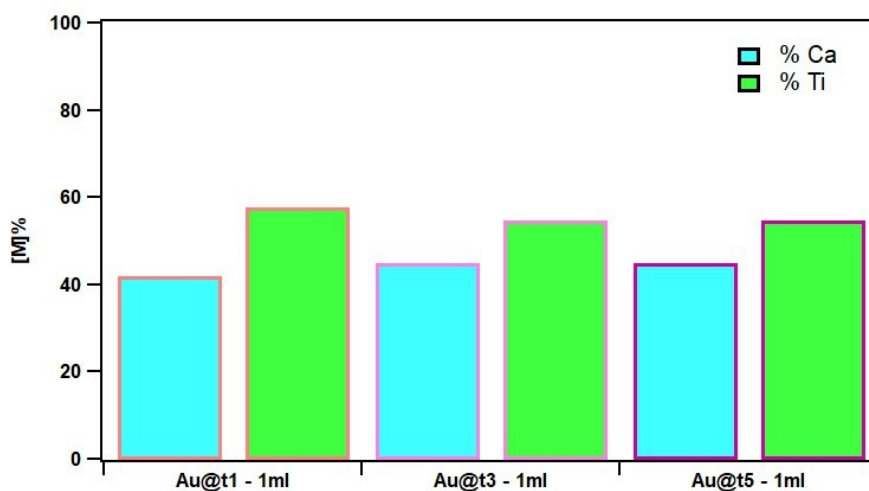


Figure S23. Experimental Ti:Ca ratio from the EDX analysis of the different samples of Au@t1.

Inductively Coupled Plasma with Mass Spectrometry (ICP-MS)

Table S10. ICP-MS data with the amount of gold incorporated in the Au@t1 materials.

	Au (mg/Kg)
Au@t1 - 1ml	187.0 ± 4
Au@t1 - 5ml	1251 ± 19
Au@t1 - 10ml	2698 ± 30

N₂ adsorption-desorption isotherms

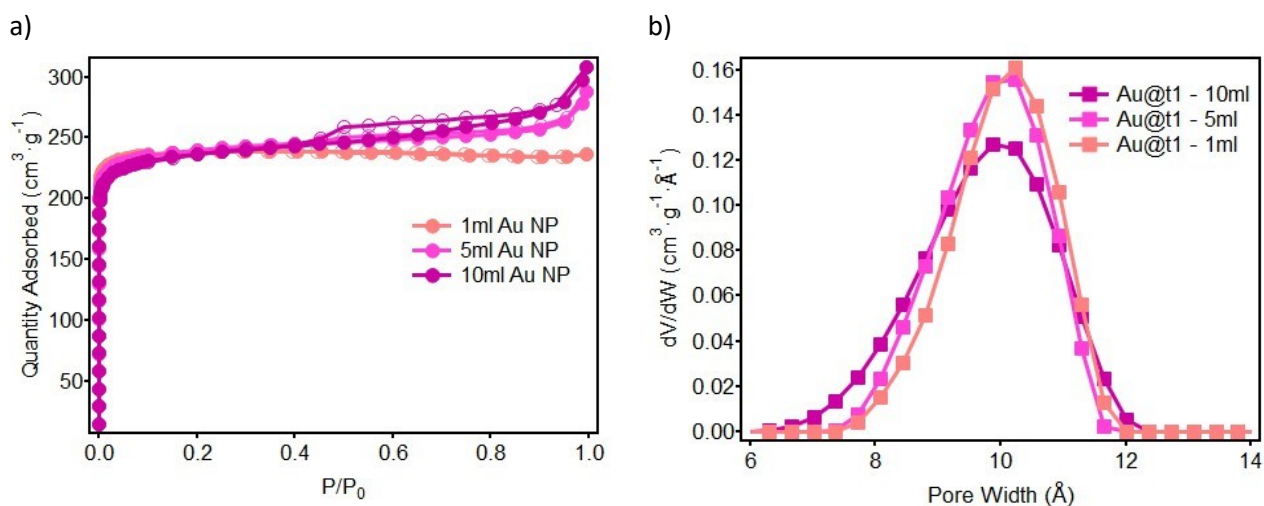


Figure S24. a) N₂ Adsorption-desorption isotherms at 77 K and b) Pore size distribution calculated.

Table S11. Summary of the N₂ adsorption isotherms at 77 K.

	BET Surface area (m ² ·g ⁻¹)	Total Pore Volume (cm ³ ·g ⁻¹)
Au@t1 - 1ml	973.2 ± 0.8	0.4
Au@t1 - 5ml	963.7 ± 0.5	0.4
Au@t1 - 10ml	941.7 ± 0.3	0.4

S4. Catalytic experiments

Two organic reactions were studied in order to test the catalytic activity of the described materials.

S4.1. Cyclotrimerization of alkynes reaction

Reaction procedure for the cyclotrimerization reaction with Au catalysts. Ethyl propiolate (1 eq, 0.01 or 0.05 mmol) and 1,2-dichlorobenzene as solvent (0.1M) were introduced in a small glass vial with a magnetic stirrer, together with the corresponding Au catalysts (typically 2 or 10 mg of the solid catalysts, 0.2 mol% Au). The vials were sealed with a small cap and allowed to react for 20 h at 120 °C. After that time, the resulting mixture was filtered and measured by gas chromatography. Products were characterized by GC-MS and NMR analyses and compared with existing literature.

Scheme S1. Gold catalysed cyclotrimerization reaction of propargyl esters.

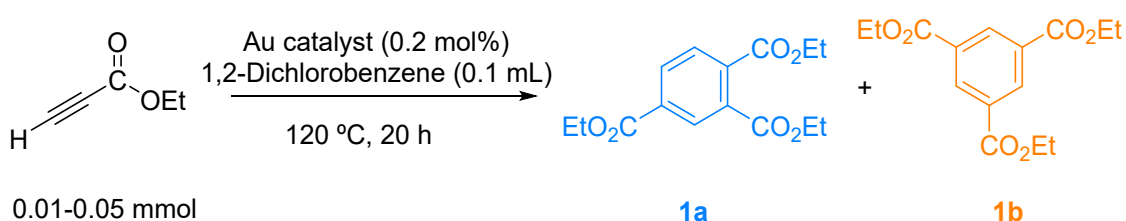


Table S12. Catalytic results of the cyclotrimerization reaction with the different Au catalysts and the blanks (performed at 0.01 mmol organic reactant scale).

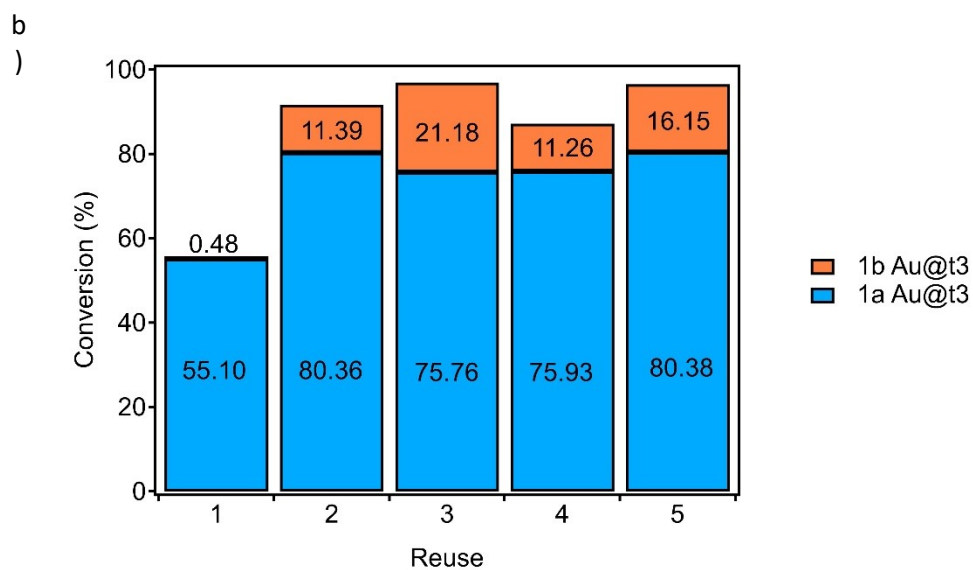
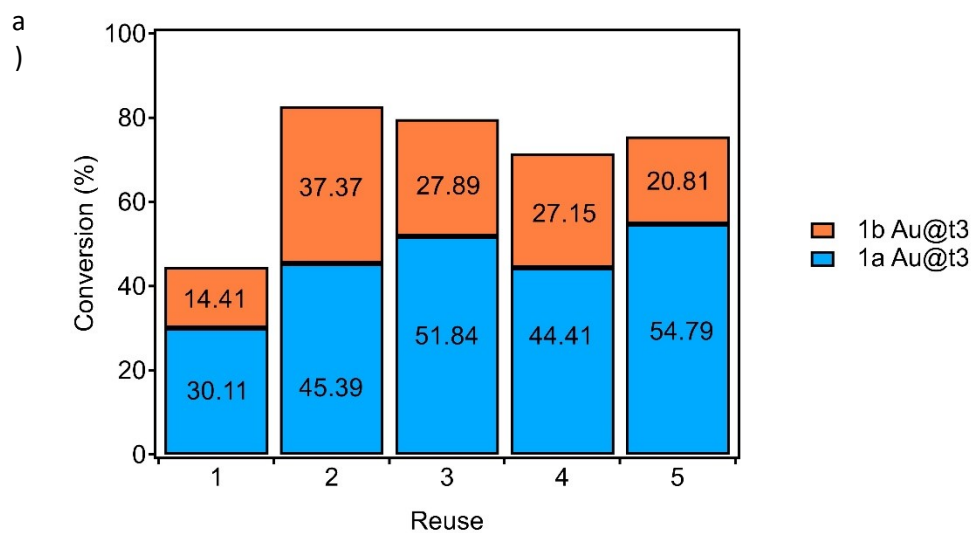
Catalyst	Conversion (%)	1a (%)	1b (%)
Blank (MOF MUV-10)	2.03	100	0
10 ml amorphous Au@t1	79.8	67	33
5 ml amorphous Au@t1	75.1	75	25
1 ml amorphous Au@t1	82.4	100	0
1 ml incipient Au@t3	57.6	96	4
1 ml fully formed Au@t5	59.5	100	0
Au NPs in MeOH	3.56	63	36

Table S13. Comparison of the catalytic results obtained with the catalyst and the most relevant metal NPs and clusters found in the literature for the cyclotrimerization reaction of propargyl esters reported here (hmds stands for 1,1,1,3,3,3-hexamethyldisilazan-2-ide). ^a After 6 uses. ^b After 5 uses. The other catalysts were not reported as reusable.

Catalyst	Metal mol%	% of surface metal atoms	Yield (%)	TON	Selectivity 1a:1b (%)	Reference
<i>Arachno</i> -[(CO) ₈ Re ₂ B ₂ H ₆]	1.2	100	85	71	6:1	4
1Pd3Au-TiO ₂ (3 nm NPs)	1	40	40	100	4:1	5
Subnanometric cobalt clusters in solution	2	100	92	41	4:1	6
Fe(hmds) ₂ / Fe NPs	1	100	69	69	99:1	6
Au-TiO ₂ (3 nm NPs)	1	40	99	1350 ^a	4:1	7
Au@t1 (20 nm NPs)	0.2	5	60	30000 ^b	10:1	this work

S4.1.1. Recyclability tests.

Typical reaction procedure for reusing. Reuses of the Au@t1-t5 solid catalysts were performed after separating the solids at the end of reaction by centrifugation and washing the solid mixture with methanol (three times) to remove excess ethyl propiolate and 1,2-dichlorobenzene, and any soluble product. Subsequently, the Au solid catalysts are dried in oven at 60 °C overnight and directly used in the next reaction.



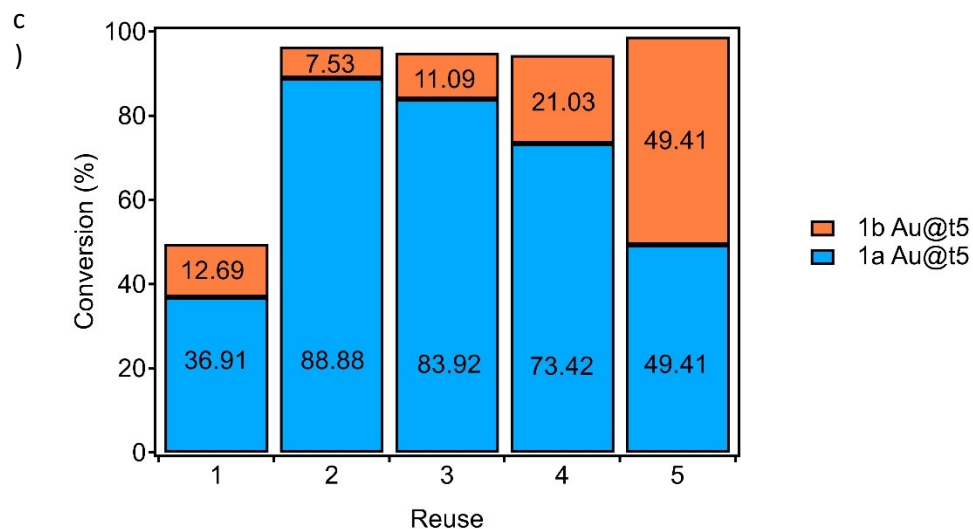
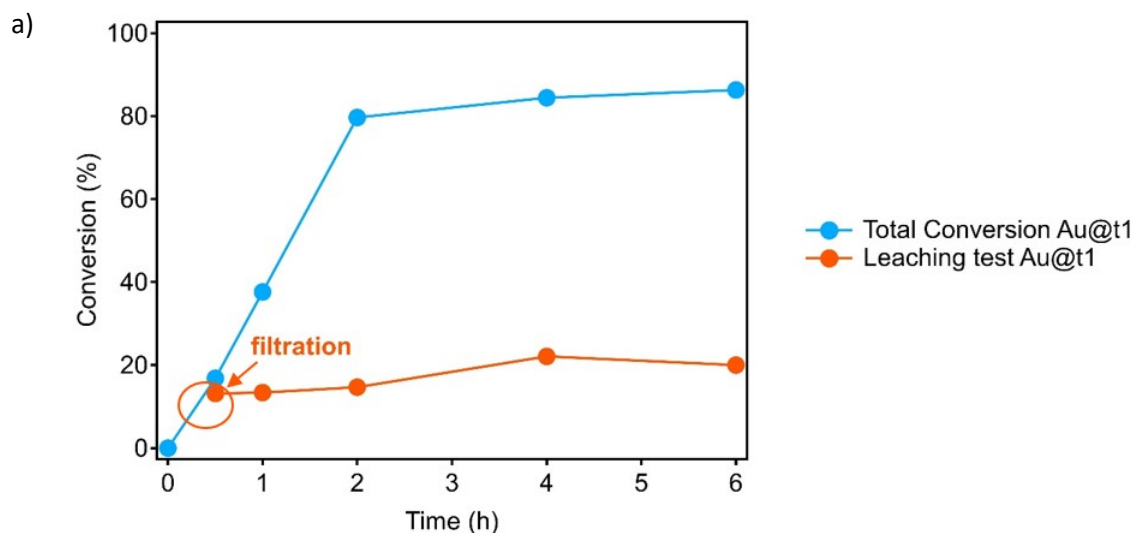


Figure S25. Recyclability tests for the cyclotrimerization reaction (performed at 0.01 mmol organic reactant scale) with a) 1 ml amorphous composite Au@t1; b) 1 ml incipient composite Au@t3 and c) 1 ml fully formed composite Au@t5.

S4.1.2. Kinetics and hot filtration studies

Kinetics and hot filtration tests were carried out in the composites where 1 ml of gold nanoparticles were added at different stages. No leaching was observed from the different materials.

Typical reaction procedure for leaching tests. Following the general reaction procedure above, the hot reaction mixture was filtered at intermediate conversion, through a 0.25 μm Teflon™ filter. Filtrates were placed into a new glass reactor equipped with a magnetic stirrer at reaction temperature, and the filtrates were periodically analyzed by gas chromatography, comparing the results obtained with the solid catalyst still in (performed at 0.01 mmol organic reactant scale).



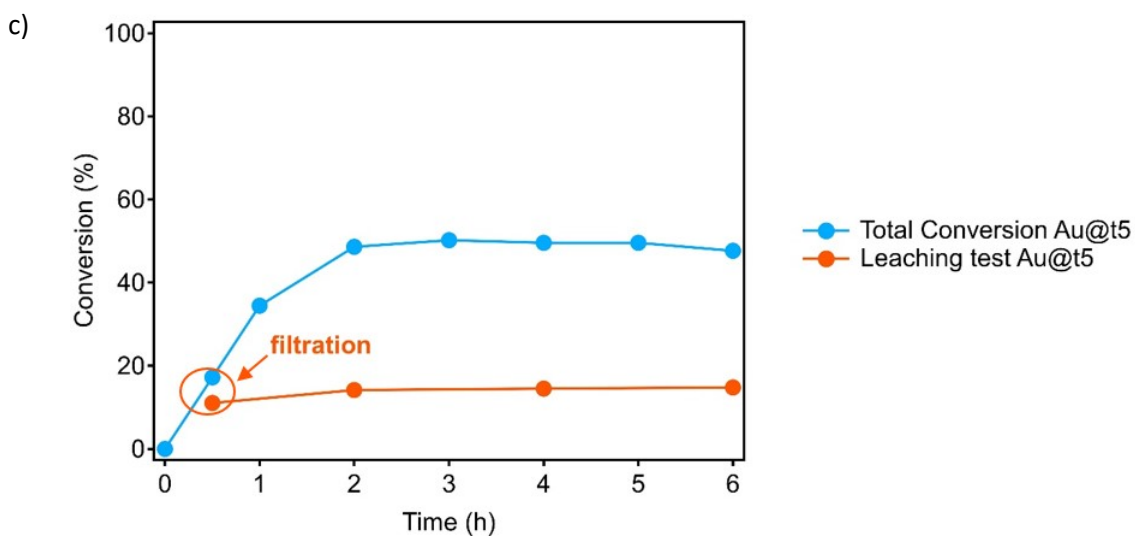
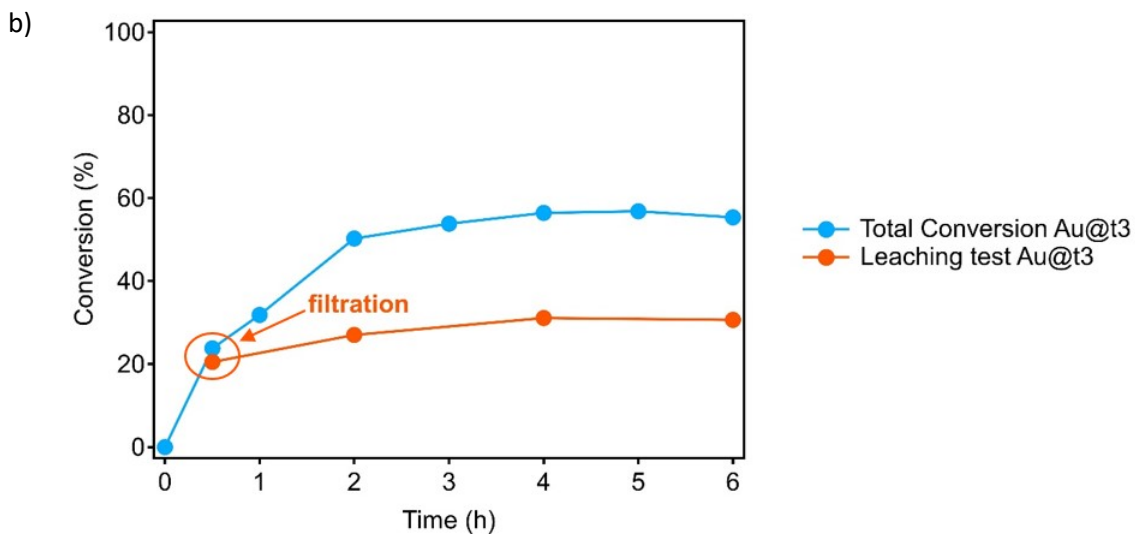


Figure S26. Hot filtration tests for the cyclotrimerization reaction with a) 1 ml amorphous composite Au@t1; b) 1 ml incipient composite Au@t3 and c) 1 ml fully formed composite Au@t5. Experiments performed at 0.01 mmol organic reactant scale.

S4.2. Hydrochlorination of alkyne reaction.

Reaction procedure for the hydrochlorination reaction with Au catalysts. Phenylacetylene (1 eq, 0.01 mmol) and a hydrogen chloride solution 0.2 mL (1M HCl in dimethyl ether) were introduced in a small glass vial with a magnetic stirrer, together with the corresponding Au catalyst (0.25 mol% Au). The vials were sealed with a small cap and allowed to react for 8 h at 80 °C. After that time, the resulting mixture is filtered and measured by gas chromatography. Products were characterized by GC-MS and NMR analyses and compared with existing literature.

Scheme S2. Gold catalysed hydrochlorination reaction.

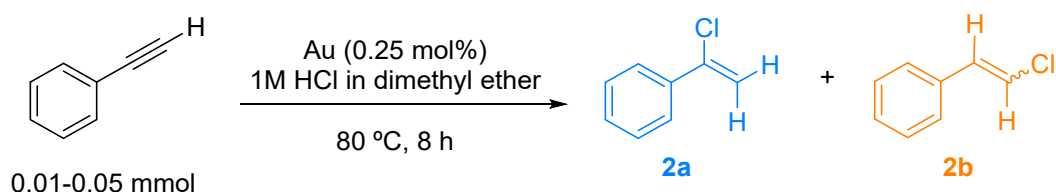


Table S14. Catalytic results for the hydrochlorination reaction of an alkyne with the different materials described in this work (performed at 0.01 mmol organic reactant scale).

Catalyst	Au mol%	Conversion (%)	2a (%)	2b (%)
Blank (MOF MUV-10)	0	6.4	60	40
No catalyst	0	0	0	0
10 ml amorphous Au@t1	2	72.8	47.6	52.4
5 ml amorphous Au@t1	1	69.4	52.2	47.8
1 ml amorphous Au@t1	0.25	70.3	66.2	33.7
1 ml incipient Au@t3	0.25	44.8	59.2	40.8
1 ml fully formed Au@t5	0.25	44.5	67.6	32.3

S4.2.1. Recyclability tests.

Typical reaction procedure for reusing. Reuses of the Au@t1-t5 solid catalysts were performed after separating the solids at the end of reaction by centrifugation and washing the solid mixture with and methanol (three times) to remove excess ethynylbenzene and hydrogen chloride solution and any soluble product. Subsequently, the Au@MUV-10 solid catalysts are dried in oven at 60°C overnight and directly use in the next reaction.

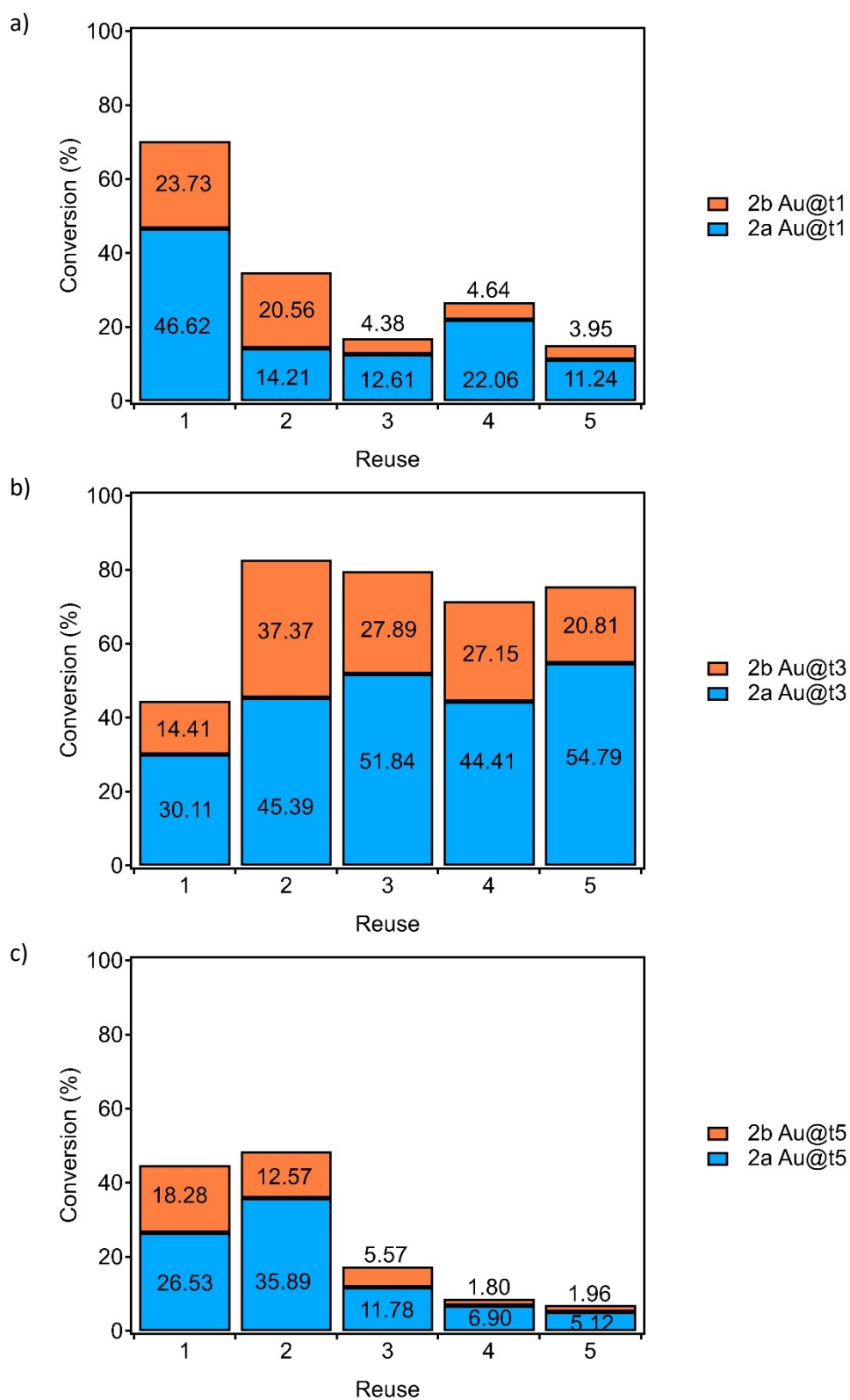


Figure S27. Recyclability tests for the hydrochlorination reaction (performed at 0.01 mmol organic reactant scale) with a) 1 ml amorphous composite Au@t1; b) 1 ml incipient composite Au@t3 and c) 1 ml fully formed composite Au@t5.

S4.2.2. Kinetics and hot filtration experiments

Typical reaction procedure for leaching tests. Following the general reaction procedure above, the hot reaction mixture was filtered at intermediate conversion, through a 0.25 μm teflon filter. Filtrates were placed into a new glass reactor equipped with a magnetic stirrer at the reaction temperature, and the filtrates were periodically analyzed by gas chromatography, comparing the results obtained with the solid catalyst still in (performed at 0.01 mmol organic reactant scale).

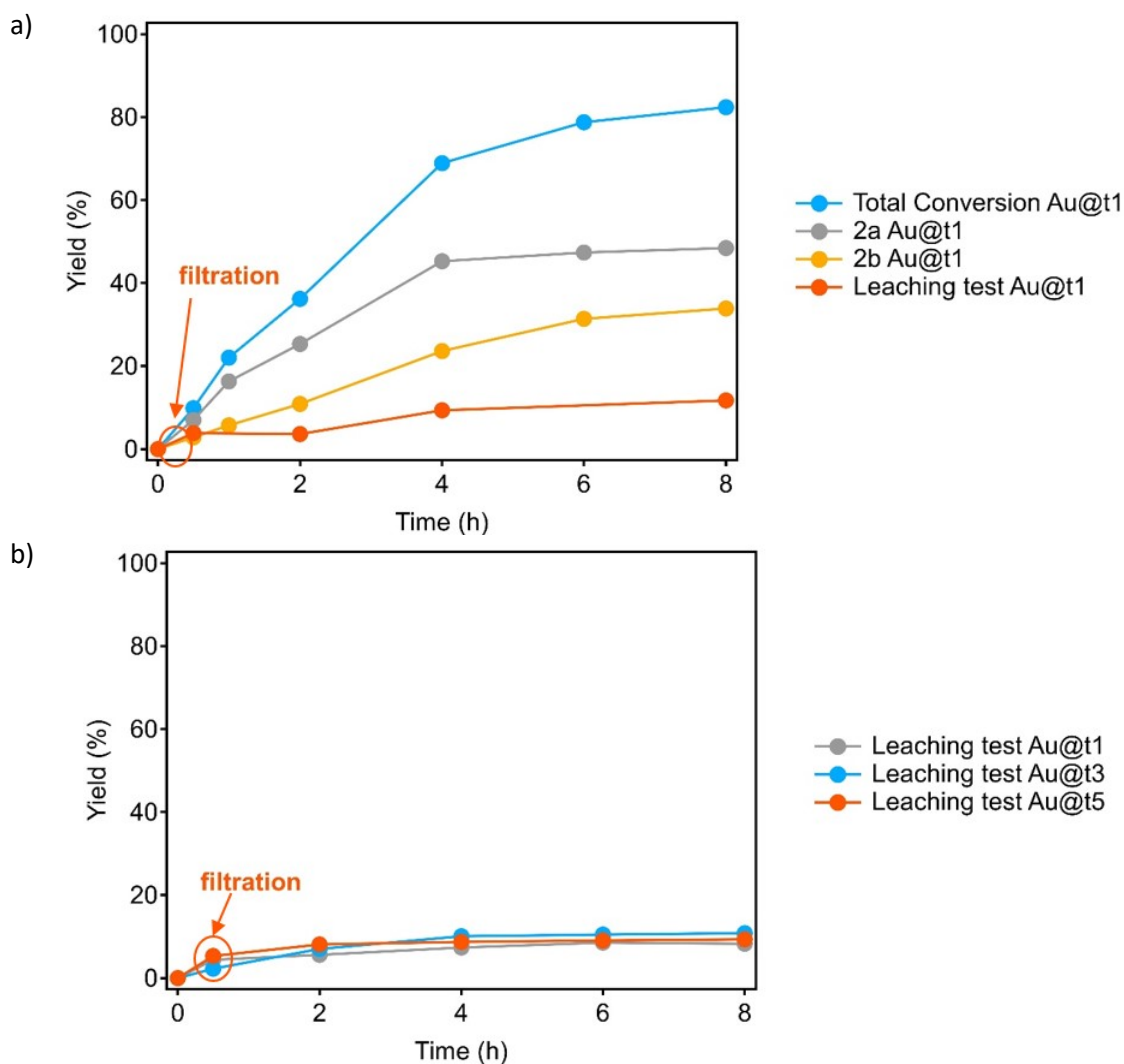


Figure S28. a) Kinetics and hot filtration test for the composite material Au@t1 (1 mol% Au) during the hydrochlorination reaction. b) Comparison with the other two materials Au@t3-t5. Experiments performed at 0.01 mmol organic reactant scale.

S5. References

1. J. Castells-Gil, N.M. Padial, N. Almora-Barrios, J. Albero, A. R. Ruiz-Salvador, J. González-Platas, H. García and C. Martí-Gastaldo, *Angew. Chem. Int. Ed.*, 2018, *130*, 8589-8593.
2. J. Turkevich, P.C. Stevenson and J. Hillier, *Discuss Faraday Soc.*, 1951, *11*, 55-75.
3. T. Hendl, M. Wuihschick, F. Kettemann, A. Birnbaum, K. Rademann and J. Polte, *Anal. Chem.*, 2014, *86*, 11115-11124.
4. V.P. Anju, S. K. Barik, B. Mondal, V. Ramkumar and S. Ghosh, *ChemPlusChem*, 2014, *79*, 546-551
5. H. Miura, Y. Tanaka, K. Nakahara, Y. Hachiya, K. Endo and T. Shishido, *Angew. Chem. Int. Ed.*, 2018, *57*, 6136-6140.
6. S. Song, C. Li, T. Liu, P. Zhang and X. Wang, *Org. Lett.*, 2021, *23*, 6925-6930.
7. J. Oliver-Meseguer, M. Boronat, A. Vidal-Moya, P. Concepción, M. A. Rivero-Crespo, A. Leyva-Pérez and A. Corma, *J. Am. Chem. Soc.*, 2018, *140*, 3215-3218.